The SNC meteorites: basaltic igneous processes on Mars

J. C. BRIDGES[1,2] & P. H. WARREN[3]

[1]*Department of Mineralogy, Natural History Museum, Cromwell Road, London SW7 5BD, UK*

[2]*Present address: Planetary and Space Sciences Research Institute, Open University, Milton Keynes MK7 6AA, UK*

(e-mail: j.bridges@open.ac.uk)

[3]*Institute of Geophysics, UCLA, Los Angeles, CA 90095, USA*

Abstract: A group of 32 meteorites, the SNC (*S*hergotty, *N*akhla, *C*hassigny) group, was derived from Mars as a product of 4–7 ejection events, probably from Tharsis and Elysium–Amazonis. The SNCs either have basaltic mineralogy or some are ultramafic cumulates crystallized from basaltic melts. The SNCs can be classified both petrographically and geochemically. We classify the shergottite SNC meteorites on the basis of their light rare earth element (LREE) depletion into highly depleted, moderately depleted and slightly depleted. The slightly depleted samples (which are mainly but not exclusively aphyric basalts) show high $\log_{10} f O_2$ values (QFM -1.0, where QFM is quartz–fayalite–magnetite). Highly depleted samples, which are mainly olivine-phyric basalts, have low $\log_{10} f O_2$ values (QFM -3.5). On the basis of mixing calculations between La/Lu and $^{87}Sr/^{86}Sr$ we favour models linking the correlation between LREE abundances and $\log_{10} f O_2$ to mantle heterogeneity rather than contamination by oxidized, LREE-rich crustal fluids. SNC chemistry in general reflects the Fe-rich mantle of Mars (which contains twice as much FeO as the Earth's mantle), the late accretion of chondritic material into the mantle, and possibly the presence of a plagioclase-rich magma ocean, which acted to variably deplete the mantle in Al. The high FeO contents of the SNC melts are associated with high melt densities (allowing the ponding of large magma bodies) and low viscosities, both of which are consistent with the large scale of many observed martian lava flows.

Of the approximately 30 000 currently known meteorites, 32 originated on Mars. The martian meteorites are also called the SNC group after three of its members: *S*hergotty, *N*akhla, *C*hassigny. They are known to form a distinct group of meteorites from a single parent body on the basis of their relatively differentiated mineralogy and chemical compositions; oxygen isotope compositions that are related to each other by mass fractionation (e.g. Clayton & Mayeda 1996); high oxidation state for meteorites ($\log f O_2$ between QFM (quartz–fayalite–magnetite) and IW (iron–wüstite); e.g. Herd 2003) and notably large range of crystallization ages (165 Ma to 4.5 Ga; Nyquist *et al.* 2001*a*).

It is the crystallization ages that first led to wide acceptance that this meteorite group was derived from a large, slowly cooled planet, Mars (e.g. McSween *et al.* 1979; Wood & Ashwal 1981). However, suggestions that some meteorites might be derived from Mars can be traced back further (e.g. Wänke 1968). Papanastassiou & Wasserburg (1974) noted that one of the SNC meteorites (Nakhla) must have been derived from an (unspecified) planetary object with some affinities to the Earth that had undergone differentiation after 3.6 Ga. The definitive link to Mars was made through comparing the composition of gases within the shock-melted glass of shergottites with the composition of the martian atmosphere determined by the *Viking* landers (Bogard & Johnson 1983).

The SNCs have a range of basaltic and ultramafic mineral assemblages (Table 1) and we show a range of new and published mineralogical and chemical data to characterize them. Sixteen of them are basaltic shergottites and eight of those have a subclassification as olivine-phyric. There are six peridotitic shergottites or 'lherzolitic shergottites', containing less plagioclase (maskelynite) than the basaltic shergottites. The nakhlites are a group of six olivine clinopyroxenites and one pyroxenite;

Chassigny and NWA2737 are dunites and ALH84001 is an orthopyroxenite. We show that the shergottites can be also be subclassified geochemically on the basis of their degree of light rare earth element (LREE) depletion. We use new trace element data to model cumulate processes in the nakhlite magma chamber. Variable patterns of depletion in incompatible elements are a feature of the SNC source melts and can be correlated with conditions of oxygen fugacity in mantle or crustal source regions. Whether the geochemical diversity amongst the SNCs is due to mantle heterogeneity related to early magma ocean crystallization or reflects mixing between mantle-derived magmas and crustal components is one of the issues we address in this paper. We present a new model to demonstrate the likelihood of a plagioclase-flotation magma ocean forming during Mars' history and compare it with the lunar example.

Spectroscopic measurements (e.g. Bandfield *et al.* 2000) show the basaltic composition of much of the martian surface; in addition, we discuss whether γ-ray, thermal emission spectroscopy (TES) data and geochemical evidence from the 1997 *Pathfinder* lander results suggest more differentiated basaltic andesites or andesites in parts of the northern lowlands as well. Regions within the northern lowlands are the most likely source of the majority of the SNCs because they have young crystallization ages equivalent to the young ages of the northern lowland terranes inferred from crater counting. The *in situ* measurements of the various landers suggest that basaltic material with some more differentiated basaltic andesites and salts dominates the uppermost surface of Mars. The SNC meteorite compositions and rock analyses from the 2004 *Spirit* and *Opportunity* landers reflect the basalt component and as we show in this paper they are related to basaltic volcanism or cumulate processes. Siderophile element abundances in SNCs are utilized to demonstrate the effects of late chondritic accretion onto the early Mars.

Table 1. *Mineralogical classification of the 32 SNC meteorites*

	Basaltic shergottites	Olivine-phyric shergottites	Peridotitic shergottites*	Nakhlites	Chassignite	Orthopyroxenite
Meteorites	Shergotty 4 kg	DaG476 2 kg	ALH77005 0.48 kg	Nakhla 10 kg	Chassigny 4 kg	ALH84001 1.9 kg
	Zagami 18 kg	Dhofar019 1.1 kg	LEW88516 13 g	Lafayette 0.8 kg	NWA2737 0.61 kg	
	EETA79001B 7.9 kg	SaU005 1.3 kg	Y793605 20 g	G. Valadares 0.16 kg		
	QUE94201 12 g	NWA1195 50 g	GRV9927 10 g	NWA817 0.1 kg		
	Los Angeles 7 kg	NWA1068 0.65 kg	Y1075 60 g	Y000593 13.7 kg		
	NWA480 30 g	Y980459 82.5 g	NWA1950 0.8 kg	NWA998 0.46 kg		
	Dhofar378 20 g	NWA2046, 63 g		MIL03346 0.72 kg		
	NWA856 0.3 kg	(EET79001A)				
	NWA1669 36 g					
Major phases (%)	aug, pig 43–70	pig 48–63	ol 40–60	aug, pig 69–85	ol 92	opx 97
	mask 22–47	ol 7–29	pig 35	ol 5–20	pig, aug 5	chr 2
	mt, sympl	mask 12–26	mask <10	ab, mt, si 5–20	chr 1	mask 1
		chr	chr <2		mask 2	
Mineral compositions						
px	$En_{1–71}Wo_{0–30}Fs_{1–94}$	$En_{66–77}Wo_{7–33}Fs_{16–31}$	$En_{69–77}Wo_{3–8}Fs_{19–21}$	$En_{37–62}Wo_{37–43}Fs_{24–41}$	$En_{49}Wo_{33}Fs_{17}$	$En_{69}Wo_3Fs_{28}$
ol		$Fo_{53–76}$	$Fo_{60–76}$	$Fo_{15–42}$	$Fo_{68–80}$	
plag/mask	$An_{39–68}$	$An_{50–70}$	$An_{45–60}$	$An_{23}Ab_{60–68}$, $An_{4–6}Ab_{20–42}Or_{52–76}$	$An_{10–60}An_{30–80}Or10$	$An_{31–37}$
Textures	Melt veins, flow alignment of grains	Porphyritic, xenocryst	Poikilitic			Cataclastic
Cumulates?	Cumulates + melt	Cumulates + melt	Cumulates	Cumulates	Cumulates	Adcumulate
Bulk Mg-no.	23–52	59–68	70	51	68	72

All of the meteorites are desert or Antarctic finds apart from the falls (i.e. seen to fall and recovered with little delay) which are: Shergotty, which fell in 1865 in Bihar State, India; Nakhla near Alexandria, Egypt, in 1911; Chassigny in Haute-Marne, France, in 1815; Zagami in Katsina province, Nigeria, in 1962. The total known masses of the meteorites in the table are given (not the pairs). NWA480 is paired with NWA1460; Y000593 with Y000749, Y000802; DaG476 with DaG489, 735, 670, 975, 1037; Los Angeles 001 with 002; SaU005 with SaU008, 051, 094, 060, 090, 120, 150, 130; NWA1068 with NWA1110, 1775. EET79001 is composed of A (olivine-phyric) and B (basaltic). Major minerals: aug, augite; pig, pigeonite; mask, maskelynite; mt, Ti-magnetite (+ ilmenite); si, silica polymorph; chr, chromite; ab, albitic plagioclase; opx, orthopyroxene. Mineral compositions from this study (pyroxene and olivine for nakhlites and chassignites; pyroxene and chromite for shergottite), Floran *et al*. (1978), McSween *et al*. (1979), Berkley *et al*. (1980), Mason (1981), Wadhwa & Crozaz (1995), McSween & Treiman (1998), Bridges & Grady (2001), Aramovich (2002), Goodrich (2003) and Mikouchi *et al*. (2005). Mineral modes from Prinz *et al*. (1974), McSween *et al*. (1979), Stolper & McSween (1979), McCoy *et al*. (1992), Mittlefehldt (1994), Lentz *et al*. (1999), Rubin *et al*. (2000), Gnos *et al*. (2002), Goodrich (2003), Meyer (2003) and Mikouchi *et al*. (2003). SaU, Sayh al Uhaymir (Oman); DaG, Dar al Gani (Libya); GRV, Grove Hills (Antarctica); LEW, Lewis Cliffs (Antarctica); ALH, Allan Hills (Antarctica); Y, Yamato (Antarctica); NWA, North West Africa (e.g. Morocco, Libya); EET, Elephant Moraine (Antarctica); Dhofar (Oman); QUE, Queen Elizabeth Range (Antarctica); MIL, Miller Range (Antarctica).
*Also referred to as the lherzolitic shergottites.

Methods

Quantitative mineral analyses (electron probe microanalysis; EPMA) of shergottites and nakhlites were made with the Cameca SX50 at the Department of Mineralogy, Natural History Museum, UK. Accelerating voltages used were 15–20 kV with 15 nA specimen current. The X-ray maps of Governador Valadares were gathered on the Cameca SX50 at 60 nA specimen current and 20 kV. The maps obtained were then processed to normalize the data and provide colour representations across the main range of elemental concentrations. We determined trace element abundances on nakhlite SNC meteorites by quadrupole-based laser ablation inductively coupled plasma mass spectrometry (LA-ICP-MS) using a NewWave Research (Fremont, USA) UP213 LA system coupled to a Thermo Elemental (Winsford, UK) PQ3 ICP-MS system with enhanced sensitivity S-option interface at the Natural History Museum, UK. Beam spot diameter within the rasters were 60–85 μm. For calibration we used the National Institute of Science and Technology (NIST) standard reference material NIST SRM612. Perkins *et al*. (1993) has provided an in-depth discussion of the LA-ICP-MS technique. REE contents were determined by normalization to Ca or Si contents previously determined by EPMA. Whole-sample REE contents of Nakhla and Y000593 were determined using the ICP-MS system in solution mode. The Y000593 and Nakhla (BM1913, 26) sample sizes were 100 mg. The samples were put into solution within platinum crucibles using 1 ml HNO_3 + 1 ml $HClO_4$ + 5 ml HF, evaporated to dryness and then redissolved in 2 ml HNO_3.

Bulk analyses of the DaG476 and SaU005 shergottites and the Y000593 and Y000749 paired nakhlites were obtained at UCLA using mainly instrumental neutron activation analysis (INAA; procedure of Warren *et al*. 1999), augmented for major elements by EPMA of fused beads (procedure of Warren & Wasson 1979).

The SNCs: petrology

The basaltic shergottites have a clearly basaltic set of mineral assemblages (augite, pigeonite, plagioclase ± olivine; Table 1). The other, ultramafic SNCs are cumulates related to basaltic magmas. The SNCs are characterized by moderate to strong shock alteration, i.e. 15–45 GPa (Nyquist *et al*. 2001*a*). This is manifested by fractures in the nakhlites and ALH84001, conversion of plagioclase to maskelynite (which is generally considered to be diaplectic glass, i.e. formed in a solid-state transformation) in the shergottites and ALH84001. The peridotites have undergone the highest degree of shock and post-shock heating up to *c*. 600 °C. Another feature of the SNCs related to shock alteration is glassy impact melts (e.g. the lithology C veins of EET79001).

Two-pyroxene geothermometry, exsolution lamellae in shergottite and nakhlite pyroxenes, and the compositions of coexisting Ti-magnetite and ilmenite all show that varying degrees of subsolidus equilibration have also taken place within many of the SNCs. For instance, ilmenite–Ti-magnetite pairs within Nakhla suggest limited equilibration at 740 °C (Reid & Bunch 1975). Two-pyroxene geothermometry for the ALH84001 orthopyroxenite suggests equilibration at 875 °C (Treiman 1995).

The SNC meteorites, in particular the nakhlites and ALH84001, also contain secondary mineral assemblages (clays, Fe-rich carbonate), which, on the basis of preterrestrial fractures and truncation by fusion crust, are known to be martian. These mineral assemblages contain a record of atmosphere–fluid–rock interaction and have been described by Bridges *et al*. (2001).

Four of the SNCs (Nakhla, Chassigny, Shergotty and Zagami) are falls; most of the remainder are Antarctic (EET, QUE, Y, ALH, GRV) and desert finds (NWA, Dhofar, DaG, SaU). Three of the SNCs have uncertain origins: Los Angeles, Governador Valadares and Lafayette. These latter meteorites were identified in a dealer's collection in Los Angeles, in Governador Valadares, Brazil, and in a university collection in Lafayette, IN, USA. The desert finds show varying degrees of terrestrial weathering such as the growth of calcite.

Basaltic shergottites

The greatest number of martian meteorites are basaltic shergottites (Tables 1 and 2). They contain two clinopyroxenes (augite and pigeonite), typically zoned towards Fe-rich rims (Fig. 1). Proportions of pyroxene vary from 70 vol% in Shergotty to 44% in QUE94201 and 43% in Los Angeles (Stolper & McSween 1979; Rubin *et al*. 2000; Warren *et al*. 2004) with the remainder mainly composed of altered plagioclase. The mineral modal abundances of the basaltic shergottites have been summarized in more detail by Goodrich (2003) as follows: pigeonite 36–45%, augite 10–34%, plagioclase (maskelynite) 22–47%, and bulk Mg-number ranges from 23 (Los Angeles) to 52 (Zagami). Hydrous amphiboles have been tentatively identified within melt inclusions (e.g. Floran *et al*. 1978; Treiman 1985; Johnson *et al*. 1991). These are calculated, on the basis of the amphibole stability, to have crystallized from melts that contained up to 1.8 wt% H_2O (Johnson *et al*. 1991; McSween & Harvey 1993). Watson *et al*. (1994) used ion probe analyses of D and H in the amphiboles to show that they actually now contain less than one-tenth of such H_2O contents. They also suggested that postcrystallization D enrichment of initially D-poor phases by martian crustal fluids with near-atmospheric D/H had occurred. It is possible that magmatic H_2O contents were diminished by shock and the initial values in the melts remain uncertain.

The basaltic shergottites are not all homogeneous samples: Zagami is composed of three different lithologies, which although all basaltic shergottite, vary in terms of pyroxene grain

Table 2. *Geochemical classification of martian meteorites*

Shergottites			Nakhlites and dunite	Orthopyroxenite
Highly depleted (HD)	Moderately depleted (MD)	Slightly depleted (SD)		
La/Lu				
0.08–0.11	0.3–0.5	0.8–1.2	3.7–5.2	0.4
Initial $^{87}Sr/^{86}Sr$ (at 175 Ma)				
0.700–0.703	0.710–0.713	0.721–0.723	all 0.704	0.722
Crystallization ages (Ma)				
300–600	all ~180	165–185	all ~1300	~4500
Sum: cosmic-ray exposure plus terrestrial ages (= presumable Mars-launch age) (Ma)				
1.0 to ~19	0.9 (EET)–4	all ~3	all ~11	~15
Known membership				
DaG476	ALH77005	Dhofar 378	Chassigny (dunite)	ALH84001
Dhofar 019	EET79001 (A/B)	Los Angeles	G. Valadares	
QUE94201	GRV99027	NWA480	Lafayette	
SaU005	LEW88516	NWA856	Nakhla	
Y980459	Y793605	NWA1068	Y000593	
		NWA1669		
		Shergotty		
		Zagami		

The La/Lu range shown for HD shergottites excludes Dhofar 019, which is heavily weathered; exclusion of other warm-desert shergottites would not affect the ranges shown. Crystallization ages, initial $^{87}Sr/^{86}Sr$, La/Lu ratios and cosmic-ray exposure ages from Nyquist *et al*. (2001*b*), Borg *et al*. (2002) and Meyer (2003).
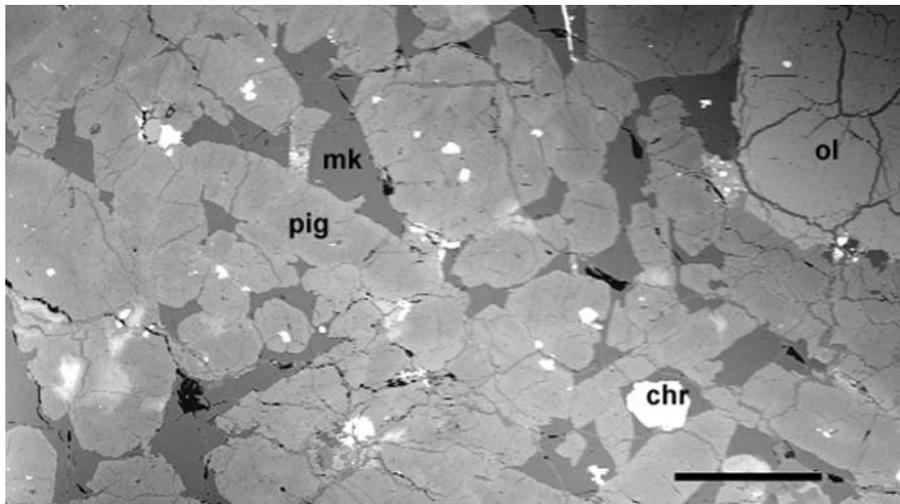

Fig. 1. Shergotty basaltic shergottite in thin section. px, clinopyroxenes (pigeonite and augite grains); mk, maskelynite; mt, magnetite. The lighter margins of the pyroxene grains are Fe-enriched rims, and this is typical of both basaltic and olivine-phyric shergottites. Black parts are holes in the section. Back-scattered electron image. Field of view 5 mm.

size (from 0.2 to *c.* 2 mm) and proportions of glassy melt (McCoy *et al.* 1992). EET79001 is composed of a basaltic lithology B, an olivine-phyric lithology A and a lesser basaltic glassy lithology C in veins and pockets, the last containing trapped martian atmospheric gases (Bogard & Johnson 1983).

Plagioclase has crystallized after the pyroxenes in all shergottites and has been altered to maskelynite through shock. Ti-magnetite, ilmenite, apatite, pyrrhotite, glass and symplectites are also present within interstitial areas.

The range of pyroxene compositions is shown in Figure 2 (and see mineral compositions of SNCs in Table 3). There is a large overall range: $En_{1-71}Wo_{0-30}Fs_{1-94}$, with Los Angeles containing the most Fe-rich pyroxenes. The other basaltic shergottites show more restricted ranges of pyroxene compositions; for instance, Shergotty augites and pigeonites are $En_{30-71}Wo_{11-34}Fs_{19-47}$. Indirect evidence for extreme Fe enrichment associated with pyroxene crystallization is shown by the presence of symplectites in some of the basaltic shergottites, e.g. Shergotty, Zagami, Los Angeles, QUE94201 (Aramovich 2002). The symplectites are believed to have formed through replacement of ferrosilite-rich pyroxene with compositions in the 'forbidden' zone of the pyroxene quadrilateral during cooling above 1000 °C for over 3 days (Lindsley *et al.* 1972). The symplectites consist of *c.* 1–10 μm sized fayalite + SiO_2 polymorphs $\pm$ hedenbergite and merrillite $Ca_9(MgFe^{2+})(PO_4)_7$ grains. The merrillite took up Mg, forcing the crystallizing pyroxene to extreme, unstable Fe-rich compositions.

Müller (1993) described augite exsolution lamellae along 001 within pigeonite and vice versa, and deduced that the Shergotty pyroxenes had cooled at 0.002 °C h^{-1} at temperatures of 1100–800 °C: a value comparable with that for large terrestrial intrusions and consistent with the relatively slow cooling at high temperatures suggested by the presence of symplectites in basaltic shergottites. We discuss the depth of origin of the shergottites in relation to magma water content in a later section.

McSween *et al.* (1996) showed that the zonation patterns of Fe enrichment towards the margins of pyroxene grains were similar to those of lunar pyroxenes that had crystallized from melts. Kring *et al.* (2003) also showed that QUE94201 pyroxene core compositions were consistent with formation from a melt with the composition of the bulk sample. Thus QUE94201 is regarded
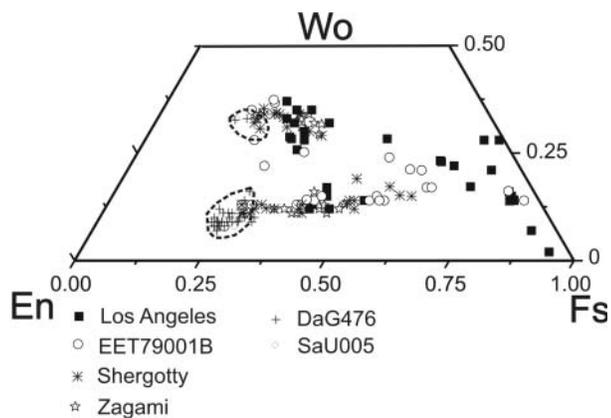

Fig. 2. Pyroxene (augite and pigeonite) compositions in basaltic shergottites and two olivine-phyric shergottites (SaU005 and DaG476) in dashed line areas. The pyroxenes are all notably Fe-enriched, with the most extreme enrichment seen in Los Angeles. The olivine-phyric shergottites have the least Fe-rich augite and pigeonite. Analyses made with Cameca SX50, Natural History Museum.

Table 3. *Mineral compositions in the SNC meteorites*

	Y000593 aug	Y000593 aug	Y000593 aug	Nakhla aug	Laf. ol	GV ol	Ch. ol	Ch. chr	GRV9927 pig	SaU005 chr	SaU005 ol	Shg pig	Shg aug	Shg mask
SiO₂	52.0	52.1	47.7	51.6	31.6	33.1	37.5	0.03	55.8	0.16	37.8	52.6	51.8	56.1
TiO₂	0.08	0.24	0.61	0.19	0.05	0.03	0.05	2.56	0.04	5.93		0.1	0.17	0.04
Al₂O₃	0.46	0.77	1.41	0.69		0.03	0.02	9.24	0.33	8.63	0.05	0.62	0.99	27.1
Cr₂O₃	0.4	0.38	0.05	0.43	0.01	0	0.16	48.5	0.47	46.4	0.08	0.47	0.6	
FeO	14.1	13.7	25.6	14.2	53.4	48.3	26.1	34.1	12.7	31.9	26.6	17	12.6	0.64
NiO		0.05	0.02	0.02	0.05	0.03	0.1			0.12				
MgO	13.2	13.3	6.03	13.4	13.7	16.6	35.6	3.65	29.3	5.02	35	21.4	16.4	0.07
MnO	0.47	0.42	0.67	0.44	1.06	0.97	0.45	0.54	0.42	0.47	0.5	0.57	0.51	0.04
CaO	19.0	19.3	17	18.9	0.13	0.52	0.09	0.01	1.31	0.08	0.29	6.7	16.1	10.8
Na₂O	0.22	0.23	0.25	0.21	0.02	0.09			0.04		0.02	0.08	0.2	5.23
K₂O	0.02		0.02	0.02	0.02			0.02			0.01		0.02	0.18
Total	99.9	100.5	99.4	100.1	100.0	99.7	100.1	98.7	100.4	98.7	100.4	99.6	99.4	100.2
En	0.38	0.38	0.19	0.38					78.5			0.6	0.47	
Fs	0.23	0.22	0.44	0.23					19			0.27	0.2	
Wo	0.39	0.40	0.37	0.39					2.5			0.14	0.33	
Fo					0.31	0.38	0.71				0.7			
Cr-no.								77.8		80.3				
Mg-no.								18.1		17				
Fe-no.								7.4		1.3				
An														52.6

Laf, Lafayette; GV, Governador Valadares; Ch., Chassigny; Shg, Shergotty. Y000593, Nakhla, Laf and GV are nakhlites; GRV9927 is a peridotitic shergottite; SaU005 is an ol-phyric shergottite. ol, olivine; pig, pigeonite; aug, augite; mask, maskelynite; chr, chromite. Atomic ratios: $En = Mg/(Ca + Mg + Fe)$; $Fs = Fe/(Ca + Mg + Fe)$; $Wo = Ca/(Ca + Mg + Fe)$; $Fo = Mg/(Mg + Fe^{2+})$; Cr-number $= 100Cr/(Cr + Al + Fe^{3+})$; Mg-number $= 100Mg/(Mg + Fe^{2+})$; Fe-number $= Fe^{3+}/(Fe^{3+} + Cr + Al)$; $An = 100Ca/(Ca + Na + K)$.

as a bulk melt composition (e.g. McSween *et al*. 1996; Wadhwa *et al*. 1998) whereas most of the other shergottites contain some cumulus pyroxene (Hale *et al*. 1999). Apart from QUE94201 and Los Angeles the shergottites also contain too high a proportion of pyroxene to have formed as 100% melts (McSween 1994). We discuss the phase relations of the SNCs and their associated melts in later sections. Evidence that Mg-rich pyroxene cores in most of the basaltic shergottites accumulated rather than crystallized *in situ* has often been taken from the preferred orientations of the pyroxene grains, which define a layered fabric. However, although the basaltic shergottites are often described as cumulates there is no compositional evidence that crystal–melt segregation or accumulation of phenocrysts had any major effect on the rock compositions. Hale *et al*. (1999) calculated the proportion of homogeneous Mg-rich cores of pyroxene within Zagami and Shergotty (14 and 19%) and suggested that this was the proportion of cumulus grains.

Mittlefehldt (1999) suggested that EET79001 lithology A was an impact melt with a hybrid composition derived from basaltic lithology B and lherzolitic cumulates. However, the impact melt model for EET79001B requires a remarkable coincidence between the age of the impact, i.e. the crystallization age of lithology B, 174 ± 3 Ma (Nyquist *et al*. 2001*b*), and the 175 ($\pm$ *c*. 10) Ma mode among regular igneous ages for shergottites. Warren & Kallemeyn (1997) cited additional weaknesses of the impact melt hypothesis, including siderophile (Au) data, the limited variety of clast types within the putative impact melt, and the gradational nature of the 'A' to 'B' contact; a constraint reinforced by the detailed petrological study of van Niekerk *et al*. (2005).

Olivine-rich shergottites

Eight of the basaltic shergottites contain up to 7–29% large (1–3 mm) olivine grains (Table 1, Fig. 1) and have been described as olivine-phyric shergottites or picritic shergottites (Gnos *et al*. 2002; Goodrich 2003). This includes lithology A of EETA79001. These shergottites also have a higher bulk Mg-number range of 59–68 (Goodrich 2003) than the basaltic shergottites and contain chromite, rather than Ti-magnetite and ilmenite, as the main oxide phase (Table 3). The olivine in SaU005 is Fo_{62-72} (this study), in EETA79001A it is Fo_{53-76} (Goodrich 2003), the larger grains having the more Mg-rich compositions. The most Mg-rich olivine of the olivine-rich shergottites is found within Y980459 (Fo_{84}) (Greshake *et al*. 2004). One of the characteristics of the SNCs is that they have relatively oxidized mineral assemblages compared with other meteorite groups. For instance, chromite cores in SaU005, DaG476 and EET79001A have $100Cr/(Cr + Al)$ atomic ratios of 74–87, $100Mg/(Mg + Fe^{2+})$ 12–36 and $100Fe^{3+}/(Fe^{3+} + Cr + Al)$ 0–5 (Bridges & Grady 2001). Pyroxenes in the olivine-phyric shergottites are more Mg-rich than in the basaltic shergottites: SaU005 and DaG476 are $En_{66-77}Wo_{7-33}Fs_{16-31}$ (Fig. 2).

McSween & Jarosewich (1993) and McSween (1994) proposed that the olivine grains were xenocrysts resulting from the mixing of peridotitic material and basaltic shergottites. However, in a study of their textures, Goodrich (2003) noted that many of the large olivine grains were compositionally zoned and subhedral, and described them as predominantly phenocrysts, which may, however, have been brought into the magma rather than crystallizing *in situ*. Uniquely for the shergottites, Y980459 contains no plagioclase or maskelynite and was inferred to have cooled rapidly upon extrusion onto the martian surface after crystal-

lization of Mg-rich cumulus phases in an underlying magma chamber (Greshake *et al*. 2004).

Peridotitic (lherzolite) shergottites

The six peridotitic shergottites have similar mineral assemblages to the olivine-phyric basaltic shergottites but contain <10 vol% maskelynite, 40–60% olivine, 9–25% pigeonite and augite; with bulk Mg-number *c*. 70 (e.g. McSween *et al*. 1979; Mason 1981; Goodrich 2003). They are cumulates with euhedral olivines typically poikilitically enclosed by pigeonites or augites up to 5 mm across. The pigeonites sometimes contain exsolutions of orthopyroxene and high-Ca pyroxene. Some peridotitic shergottites also show a clearly defined alignment of cumulate grains (Berkley & Keil 1981). Mineral compositions of the peridotites overlap those of olivine-phyric shergottites, with a range of olivine compositions of Fo_{60-76} (McSween & Treiman 1998). The peridotitic shergottites are often referred to as the lherzolitic shergottites but as they lack significant quantities of orthopyroxene the term peridotite is more accurate. Chromite has similar compositional ranges and Fe^{3+} contents to those in the olivine-phyric shergottites.

Nakhlites and Chassigny

The seven nakhlites are cumulate olivine clinopyroxenites composed of augite, Fe-rich olivine and mesostasis (Tables 1 and 3; Fig. 3). One of the nakhlites, MIL03346, is an olivine-free clinopyroxenite. Lentz *et al*. (1999) published modal abundances of Nakhla, Lafayette and Governador Valadares showing that they contained similar proportions of the main mineral phases: olivine 5–20%, pyroxene 69–85%, mesostasis 5–13%. An average olivine content based on our own studies of nakhlite sections (Nakhla, Lafayette, Governador Valadares, Y000593) is consistently *c*. 10%. However, NWA817 has a distinctly higher proportion of mesostasis than the other nakhlites (20%, Sautter *et al*. 2002; Mikouchi *et al*. 2003). Mesostasis in the nakhlites is composed of plagioclase and alkali feldspar dendritic grains,
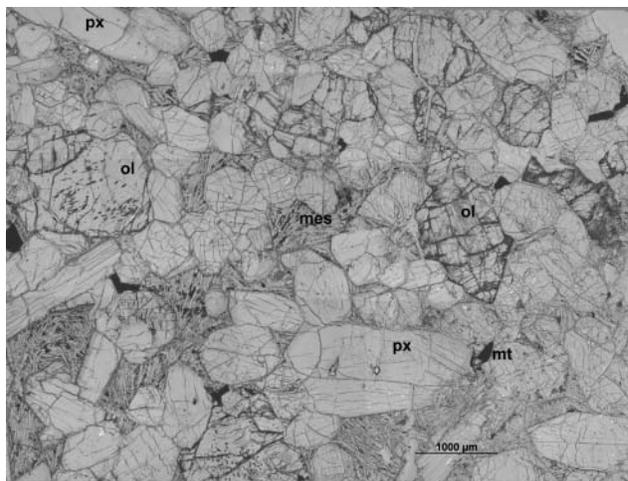

Fig. 3. Y000749 nakhlite (a meteorite paired with Y000593; that is, they are thought to be part of the same meteorite when it fell) in thin section. Radiating laths of plagioclase are seen in the mesostasis. Planar fractures, running NE–SW, are present in the marked, large olivine grain in the centre–right of the image, and these are a feature of shock metamorphism. ol, olivine; px, pyroxene (augite); mes, mesostasis; mt, Ti-magnetite. Plane-polarized view, scale bar represents 1000 µm.

pyroxene dendrites, glassy mesostasis, Ti-magnetite and ilmenite, silica polymorphs, chlorapatite and sulphides, together with occasional baddeleyite and secondary mineral assemblages such as siderite (Bridges & Grady 2000). The presence of silica polymorphs shows the silica-oversaturated nature of the mesostasis. Unlike Chassigny (see below) the augite cores (mainly within the range $En_{0.37-0.62}Wo_{0.37-0.43}Fs_{0.24-0.41}$) and olivine ($Fo_{14-44}$) studied here have not been equilibrated to a great degree (Fig. 4). However, the augite rims are zoned to Fe-rich compositions, hedenbergite in NWA817 and MIL03346. NWA817 and MIL03346 olivine also shows the greatest range of olivine compositions of the nakhlite samples, including some zonation within individual grains, from Fo_9 to Fo_{44} (Sautter et al. 2002; McKay & Schwandt 2005).

The presence of radiating plagioclase dendrites in the mesostasis (Fig. 3) may require that the final cooling of interstitial liquid took place rapidly in a quenching event, subsequent to the slower cooling associated with accumulation of the augite and olivine grains. Magmatic or melt inclusions (predominantly fine-grained pyroxene and feldspar, glass, apatite, ilmenite inter-

growths) in the nakhlites, especially within olivines, have been used to reconstruct parent melt compositions (e.g. Treiman 1993) and we consider this further in relation to phase equilibria of martian basalts in a later section.

Chassigny is a cumulate dunite, having >90% olivine. The remainder is composed of augite and low-Ca pyroxene (occasionally poikilitically enclosing the olivine), plagioclase, minor orthoclase and chromite, and melt inclusions with H_2O-bearing kaersutite amphibole, biotite and glass (Floran et al. 1978; Johnson et al. 1991). The olivine (Fo_{68-71}) and chromite (Mg-number 12–19) have relatively narrow compositional ranges showing equilibration at 1150–1230 °C (Wadhwa & Crozaz 1995). However, there is evidence (Floran et al. 1978) for compositional heterogeneity in the chromite analyses. This sample has similar crystallization and ejection ages to the nakhlites and so is often regarded as having originated as part of the same set of igneous rocks on Mars. Both the nakhlites and Chassigny did form from LREE-enriched magmas but Wadhwa & Crozaz (1995) suggested that the differing slopes of the REE profiles are not consistent with formation from the same melt. Despite the presumed close proximity of their origin (on the basis of their very close ejection ages) there is no clear model to relate the magmatic history of the nakhlites and Chassigny.

The second chassignite is NWA2737, which contains 89% homogeneous olivine. The NWA2737 mineral assemblage is closely similar to that of Chassigny except that the minerals are more Mg-rich; for example, olivine is Fo_{79-80} (Mikouchi et al. 2005).

ALH84001

ALH84001 is an orthopyroxenite with a cataclastic texture. Orthopyroxene grains are up to 6 mm in diameter, occupying 97% of the rock, with maskelynite (mainly An_{31-37}), chromite, augite, apatite and pyrite representing the remnants of a small amount of trapped interstitial melt. Mittlefehldt (1994) proposed that it was a cumulate on the basis of its near monomineralic, equilibrated nature, coarse grain size and homogeneous pyroxene composition (mean is $Fs_{28}Wo_3En_{69}$). Its small degree of trapped melt means that it can be considered an adcumulate. Chromite in ALH84001 has $100Fe^{3+}/(Fe^{3+} + Cr + Al)$ of 4.5–10 (Bridges & Grady 2001). ALH84001 is particularly famous for its secondary carbonate 'rosettes' (e.g. Mittlefehldt 1994; McKay et al. 1996; Bridges et al. 2001).

Physical parameters

The calculated room-temperature densities for SNC meteorites vary from 3.59 g cm^{-3} for the Chassigny dunite to 3.18 g cm^{-3} for EET79001B basaltic shergottite (Lodders 1998). The density of peridotite LEW88516 is 3.39 g cm^{-3} and that of Nakhla is 3.33 g cm^{-3}. The high FeO contents of the SNC melts are associated with high magma densities relative to a martian crustal density of c. 3.0 g cm^{-3}, allowing the ponding of large magma bodies. This and low viscosities are both consistent with the scale and morphology of many observed martian lava flows. In Table 4 we show our calculated melt densities at a liquidus temperature of 1200 °C and 1.5 kbar for the basaltic shergottites, and the *Pathfinder*, *Spirit* and *Opportunity* results. The low-pressure density of a silicate melt can be calculated to good precision based on its composition and the partial molar volumes of its constituent oxides (Lange & Carmichael 1990). The 1.5 kbar pressure is equivalent to 10 km depth (Turcotte & Schubert 1982), i.e. upper to mid-crustal thickness for much of
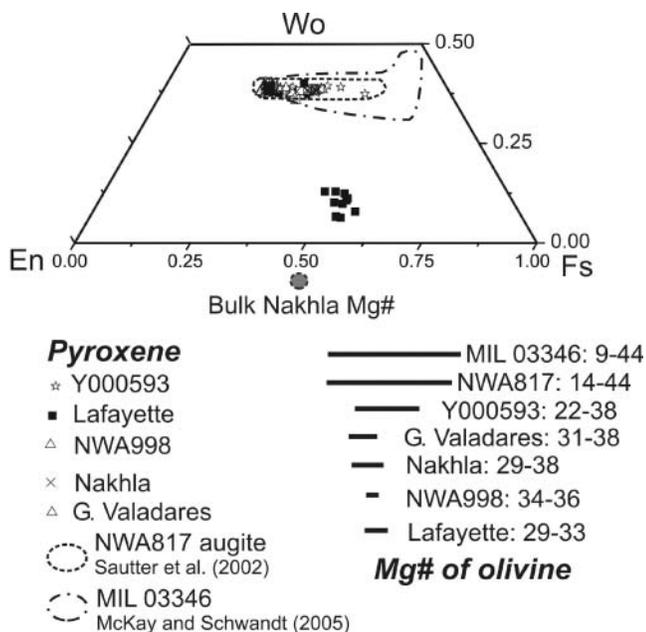

Fig. 4. Pyroxene and olivine compositions in the nakhlites. The main mineral phase in the nakhlites is an Fe-rich augite ($En_{0.37-0.62}Wo_{0.37-0.43}Fs_{0.24-0.41}$) with lesser amounts of pigeonite ($En_{48-54}Wo_{6-13}Fs_{35-39}$). There is little discernible compositional variation between four of the nakhlites (Nakhla, Lafayette, Governador Valadares, NWA998). However, Y000593 and NWA817 have the most Fe-rich augite core compositions, extending to $Fs_{0.4}$, indicating that they have more fractionated assemblages. The arrow indicates the zonation of the augite rims towards hedenbergite-like compositions; this is most extreme in NWA817 augite. NWA817 also has the greatest range of olivine compositions (Fo_{14-44}) suggesting that it has undergone the least equilibration. Olivine grain compositions are plotted beneath the pyroxene quadrilateral. Their Mg-number ratios are not in equilibrium with the pyroxene compositions or with the bulk Mg-number of Nakhla (also plotted, 0.5) and this feature may be due to late crystallization of the olivine relative to the augite cores (e.g. see Fig. 9). The pyroxene and olivine compositions are from this study, apart from the Y000593 olivine (Mikouchi et al. 2003), the NWA817 augite, rims and olivine data (Sautter et al. 2002), and MIL03346 olivine and pyroxene (McKay & Schwandt 2005).

Table 4. *Major element compositions of martian basalts, andesite and cumulates*

	SiO_2	TiO_2	Al_2O_3	FeO	MnO	MgO	CaO	Na_2O	K_2O	P_2O_5	SO_3	H_2O	Al_2O_3/CaO	Melt ρ
Pathfinder soil-free[1]	57.7	0.5	12.3	14.2	0.5	0.8	6.7	4.2	1.2	0.4			1.8	2.61
Humphrey[2]	46.1	0.52	10.6	18.0	0.39	12.2	7.7	2.59	0.06	0.56			1.4	2.85
Bounce[2]	50.8	0.78	10.1	15.5	0.43	6.5	12.5	1.25	0.1	0.95			0.8	2.79
Viking soil[3]	47.0	0.7	8.0	17.7		6.4	6.4	n.d.	0.0	n.d.	7.9			
Barnacle[4]	53.9	0.6	12.8	17.1	0.3	2.1	5.7	3.2	1.1	0.7	2.0	0.3	2.2	2.70
Yogi	45.7	0.7	10.8	17.8	0.4	5.1	6.3	4.7	0.7	0.5	4.3	3.4	1.7	2.88
Wedge	47.2	0.7	11.3	18.3	0.3	4.0	6.8	4.8	0.8	0.5	3.0	1.5	1.7	2.87
Shark	51.5	0.5	10.2	15.1	0.4	3.7	7.3	3.4	0.8	0.4	1.6	4.3	1.4	2.80
Half Dome	50.0	0.7	12.3	17.9	0.4	3.4	6.0	4.0	1.0	0.6	3.0	0.1	2.1	2.84
Peridotite shergottites[5]														
ALH77005	42.4	0.39	2.9	20.1	0.45	28.2	3.2	0.47	0.03	0.4			0.9	
LEW88516	46	0.39	3.31	19	0.49	25	4.2	0.56	0.029	0.39			0.8	
Y793605	45.4	0.35	2.32	19.7	0.48	26.2	4.06	0.36	0.025				0.6	
Basaltic shergottites														
Los Angeles	49.1	1.3	11.2	21.2	0.45	3.53	9.95	2.22	0.24	0.66			1.1	2.84
EET79001B	49.4	1.18	11.2	17.4	0.43	6.6	10.8	1.74	0.08	1.28			1.0	2.82
Shergotty	51.3	0.82	6.88	19.4	0.52	9.3	9.6	1.39	0.17	0.67		0.03	0.7	2.84
QUE94201	47.9	1.84	11	18.5	0.45	6.25	11.4	1.58	0.05				1.0	2.85
Zagami	50.5	0.79	6.05	18.1	0.5	11.3	10.5	1.23	0.14	0.5		0.03	0.6	2.85
Dhofar019	45.5	0.6	6.7	17.9	0.5	14.6	9.3	0.7	0.05	0.4			0.7	2.90
Ol-phyric shergottites														
NWA1068	47.7	0.8	5.6	20.5	0.5	16.5	7.9	1.1	0.2				0.7	
DaG476	47.2	0.4	4.2	16.5	0.4	19.4	7.8	0.6	0.03	0.5			0.5	
SaU005	47.2	0.42	4.5	18.3	0.5	20.5	5.7	n.d.	n.d.	0.3			0.8	
EET79001A	49.9	0.7	5.91	18.4	0.48	16.1	7.26	0.86	0.04	0.6			0.8	
Nakhlites														
Nakhla	48.6	0.34	1.68	20.6	0.49	12.1	14.7	0.46	0.13	0.03		0.06	0.1	
Lafayette	46.9	0.42	2.47	21.6	0.50	12.9	13.4	0.40	0.11	0.45		0.19	0.2	
Nakhlite melt[6]	50.2	1.0	8.6	19.1	0.4	4.0	11.9	1.2	2.8	0.7			0.7	2.80
Mars mantle[7]	43.7		3.1	18.7	0.1	31.5	2.5	0.5					1.2	
Earth mantle	44.5	0.2	3.6	8.1	0.1	39.2	3.4	0.3					1.1	
Terrestrial basalt[8]	49.7	0.72	16.4	7.9	0.12	10.1	13.2	2.00	0.01	n.d.			1.2	2.71
Andesite[9]	57.9	0.87	17.0	7.0	0.14	3.31	6.8	3.5	1.6	0.21			2.5	2.56

n.d., not determined.

[1]*Pathfinder* soil-free rock (Foley *et al.* 2003).

[2]Humphrey and Bounce Rocks are from Gusev (*Spirit*) and Meridiani (*Opportunity*) 2004 landing sites (McSween *et al.* 2004; Zipfel *et al.* 2004).

[3]Viking soil composition (Clark *et al.* 1982).

[4]*Pathfinder* rock compositions using the recalibration of Foley *et al.* (2003). Here we have presented them on a soil-free basis (i.e. normalized to 0 wt% SO_3) and H_2O contents consistent with andesites (i.e. ≤1 wt% H_2O).

[5]Meteorite data from compilation by Lodders (1998), apart from DaG476 (Folco *et al.* 2000), SaU005 (Dreibus *et al.* 2000), Los Angeles (Rubin *et al.* 2000).

[6]Nakhla parental magma (Treiman 1993).

[7]Mars and Earth mantle compositions (Bertka & Fei 1998).

[8]Ocean floor basalt (Basaltic Volcanism Study Project 1981).

[9]Terrestrial andesite from Cox *et al.* (1979). Melt density (ρ) in g cm^{-3} calculated for 1200 °C liquidus at 1.5 kbar based on partial molar volumes of its constituent oxides (Lange & Carmichael 1990).

Mars. These data show the expected lower densities for the basaltic andesitic-like rocks from *Pathfinder* (e.g. 2.61–2.88 g cm^{-3} compared with the basalts): Humphrey's melt has a density of 2.85 g cm^{-3} and the basaltic shergottite predicted melts a density of 2.82–2.90 g cm^{-3}. The nakhlite parent melt NK93 (Treiman 1993) has a density of 2.80 g cm^{-3}. Further details of the melt density calculations are available from the authors. The estimated viscosity range for crystal-free, hydrous SNC melts is 0.1–30 N s m^{-2} (Harvey *et al.* 1993). However, the presence of entrained cumulate crystals, as are seen in the shergottites, may act to increase the viscosity by a factor of 10 (Basaltic Volcanism Study Project 1981).

The SNCs: geochemistry

Geochemical classification of the shergottites

As discussed above, shergottites are usually subclassified on mineralogical grounds. A separate yet equally valid way of subclassifying shergottites is based on REE geochemistry (Table 5, Fig. 5). There are again three groups, which we here define as highly depleted (HD) shergottites, moderately depleted (MD) shergottites, and slightly depleted (SD) shergottites. Even the SD shergottites (which constitute the most numerous subclass) are in some respects depleted compared with chondrites, but the depletions are only very mild in comparison with HD shergottites. These geochemical subclasses correlate only loosely with the mineralogical subclasses. Most of the HD shergottites are olivine-phyric, but QUE94201 is a basaltic shergottite (Wadhwa *et al.* 1998; Kring *et al.* 2003). Most of the MD shergottites are cumulate peridotites, but EET79001 contains both basaltic and olivine-phyric MD lithologies. Most of the SD shergottites are basaltic without conspicuous phenocrysts, except NWA1068/1110, which is olivine-phyric (Barrat *et al.* 2002).

'Depleted' refers to the many elements that behave incompatibly with respect to major minerals during igneous differentiation. Exemplary incompatible elements include Th, U, Ba, and La. The ratio La/Lu is particularly diagnostic. Figure 5 shows CI chondrite-normalized REE patterns for a representative selection of shergottites. The depleted subtype have La/Lu consistently close to 0.12 × CI, whereas the SD subtype have La/Lu consistently close to 1.0 × CI. Despite their cumulate nature, the peridotitic shergottites have REE patterns (including La/Lu) lower than but roughly parallel to the patterns of their parent melts (Wadhwa *et al.* 1994). For comparison, mid-ocean-ridge basalts, which represent the major depleted reservoir within the Earth's mantle, typically have La/Lu *c.* 0.6 × CI (Basaltic Volcanism Study Project 1981). In a later section we demonstrate that these trace element signatures of highly diverse extents of depletion are paralleled by variations in initial ^{87}Sr/^{86}Sr ratios (Borg *et al.* 2002). The systematic depletion variations among shergottites tend to correlate, but only in a loose way, with key mineralogical traits. To assume that depletion or enrichment is a reliable predictor of mineralogical subclass or vice versa (Goodrich 2003; Herd 2003) can be a mistake.

Whole-rock and melt compositions

The compositions of the SNC group are similar to those of terrestrial igneous rocks in some respects. Stolper (1979) demonstrated that the siderophile and volatile trace element abundances of basaltic shergottites differ from those of terrestrial basalts by less than a factor of 10. The clearest difference in major element composition between the SNC meteorites and terrestrial igneous

rocks is the high Fe contents of the martian samples. Fe, expressed as FeO, ranges from 17.3 wt% for ALH84001 to 27 wt% for Chassigny. QUE94201 has 18.5 wt% FeO (Table 4). In contrast, typical terrestrial ocean-floor basalts and andesites have <10 wt% FeO. The SNCs have also often been considered to show Al depletion, having Al_2O_3 contents of 0.7 wt% (Chassigny dunite) to 11 wt% for the basaltic shergottites QUE94201 and EETA79001B (Lodders 1998). In Figure 6 the plots of CaO v. MgO and Al_2O_3 v. MgO show the generally low Al_2O_3 contents and similar CaO of most the SNCs compared with terrestrial basalts, but the *Pathfinder* basaltic andesites (discussed below) and *Spirit* and *Opportunity* basalt analyses do not exhibit notable Al depletion. In Table 4, the *Pathfinder*, *Opportunity* and *Spirit* results show Al_2O_3/CaO ratios similar to those for terrestrial basalts.

The bulk contents of H_2O in the SNC meteorites are low (e.g. 300 μg g^{-1} for Shergotty; Lodders 1998). The nakhlites have higher H_2O contents but these are a result of alteration processes on the martian surface. Dann *et al.* (2001) reported the results of phase equilibria experiments on Shergotty compositions. They suggested that elevated H_2O pressures *c.* 1.8 wt% were necessary for their melts to crystallize pigeonite and augite as liquidus phases at magmatic temperatures of 1000–1200 °C. If this is the case then the shergottite magma must have lost the majority of its water during ascent and prior to final crystallization. This melt water content is anomalous because the H_2O content of the martian mantle is considered to be <300 μg g^{-1} (Lodders & Fegley 1997) and therefore some form of crustal contamination associated with the addition of water into the melt has been considered necessary by various workers. Crystallization of the basaltic shergottite pyroxene cores commenced slowly at depth from H_2O-bearing melts (e.g. 4–6 km, 1.8 wt% H_2O) and was followed by more rapid crystallization of the Fe-rich rims (and in the case of Y980459 the entire matrix) in a near-surface intrusive or extrusive setting (Lentz *et al.* 2001; Beck *et al.* 2004; Greshake *et al.* 2004).

The SNC group contains both melt compositions (e.g. QUE94201) and cumulates (e.g. the nakhlites, Shergotty). In the following sections we consider melt major element compositions and relate them to the *Pathfinder*, *Spirit* and *Opportunity in situ* analyses of igneous rocks.

Basalts and basaltic andesites on Mars. The recalibration and processing of the *Pathfinder* data to remove the effects of dust cover have been described by Wänke *et al.* (2001) and Foley *et al.* (2003). Foley *et al.* used the combined alpha, proton and X-ray modes and so this may be considered the more comprehensive dataset. They demonstrated that the *Pathfinder* rock analyses contained up to 4 wt% H_2O, suggesting that alteration rinds were sampled. The *Pathfinder* soil-free rock recalculated analysis of Foley *et al.* has high SiO_2 (57.7 wt%), high K_2O (1.20 wt%) and low MgO (0.8 wt%), corresponding to terrestrial andesites or basaltic andesites (Figs 6 and 7). However, the direct evidence for olivine and pyroxene grains (i.e. igneous mineralogy) identified in basalts at Gusev by the *Spirit*lander is lacking for the *Pathfinder* analyses. Therefore the classification of *Pathfinder* rocks as basaltic andesites still has some uncertainty, with the possibility remaining that the high alkali contents are a result of unidentified contamination by dust or alteration material, or even that the rocks are not igneous (McSween *et al.* 1999; Foley *et al.* 2003).

In contrast, the basaltic shergottites (Lodders 1998) have *c.* 48–51 wt% SiO_2, <0.2 wt% K_2O and 6–16 wt% MgO, and, despite their low Al_2O_3 and high FeO contents discussed above,

Table 5. *Bulk compositions of martian meteorites determined at UCLA by INAA, augmented (for major elements) by EPMA of fused beads*

	Mass (mg)	Na (mg g⁻¹)	Mg (mg g⁻¹)	Al (mg g⁻¹)	Si (mg g⁻¹)	K (mg g⁻¹)	Ca (mg g⁻¹)	Sc (µg g⁻¹)	Ti (mg g⁻¹)	V (µg g⁻¹)	Cr (mg g⁻¹)	Mn (mg g⁻¹)	Fe (mg g⁻¹)	Co (µg g⁻¹)	Ni (µg g⁻¹)	Zn (µg g⁻¹)	Ga (µg g⁻¹)	As (µg g⁻¹)	Se (µg g⁻¹)	Br (µg g⁻¹)	Rb (µg g⁻¹)	Sr (µg g⁻¹)
DaG735-A	430	3.7	99	27	233	0.55	58	32.5	2.8	190	4.98	3.3	124	51.1	225	48	8.1	0.24	0.57	1.7	<7	67
Notable uncertainties																		14%	19%			
DaG735-B	330	3.9	101	28	238	0.51	56	33.8	2.4	180	4.94	3.5	125	54.4	239	56	8.1	<0.5	0.41	2.4	<4	90
Notable uncertainties																			27%			8%
SaU005	254	4.9	117	26	220	0.23	43	34	2.4	190	5.93	3.5	133	55.5	288	49	8.8	0.56	0.38	1.6	<3.1	47
Notable uncertainties						8%												8%	24%			
Y000593	470	4.7	65	12.3	233	1.32	105	61	2.7	200	1.82	4	157	47.6	66	68	3.4	<0.11	0.25	1.2	<4	75
Notable uncertainties																	12%		25%			8%
Y000749	590	3.9	68	10.2	226	1.2	96	56	2.1	160	1.66	4.2	175	52.3	68	81	2.3	<0.15	0.22	1.1	<4	70
Notable uncertainties																	15%		30%			14%

	Mass (mg)	Zr (µg g⁻¹)	Sb (ng g⁻¹)	Cs (ng g⁻¹)	Ba (µg g⁻¹)	La (µg g⁻¹)	Ce (µg g⁻¹)	Nd (µg g⁻¹)	Sm (µg g⁻¹)	Eu (µg g⁻¹)	Tb (µg g⁻¹)	Dy (µg g⁻¹)	Ho (µg g⁻¹)	Yb (µg g⁻¹)	Lu (µg g⁻¹)	Hf (µg g⁻¹)	Ta (µg g⁻¹)	Ir (ng g⁻¹)	Au (ng g⁻¹)	Th (µg g⁻¹)	U (µg g⁻¹)
DaG735-A	430	<30	15	<40	55	0.15	0.6	<0.43	0.38	0.22	0.23	1.8	0.28	0.84	0.13	0.4	<0.02	1.9	1.1	<0.050	[0.068]
Notable uncertainties			25%				9%					20%						20%	21%		
DaG735-B	330	<50	<50	<70	[210]	[0.56]	[0.85]	<0.81	0.45	0.22	0.21	<3.6	0.33	0.84	0.13	0.34	<0.02	1.8	0.9	<0.055	[0.104]
Notable uncertainties							12%											25%	40%		8%
SaU005	254	<24	<30	76	15	0.13	<0.8	<0.8	0.45	0.26	0.23	1.7	0.29	0.91	0.14	0.48	0.041	13	1.5	<0.061	[0.059]
Notable uncertainties				16%	24%							18%					14%		12%		15%
Y000593	470	<40	<30	340	60	3.4	7.8	5.1	1.19	0.36	0.19	<2	0.22	0.51	0.071	0.39	0.13	<2	<1	0.25	0.07
Notable uncertainties					16%																16%
Y000749	590	<50	<30	180	40	2.6	6.2	4.1	0.97	0.3	0.15	<2	0.21	0.48	0.067	0.32	0.1	<2	<0.3	0.2	0.06
Notable uncertainties					21%								13%								20%

A few data are shown in square brackets because the concentrations appear to reflect major contamination associated with warm–desert weathering. Notable uncertainties are uncertainties in INAA counting statistics that are large in comparison with 70% confidence levels (i.e. 'normal' for moderate to high concentrations).
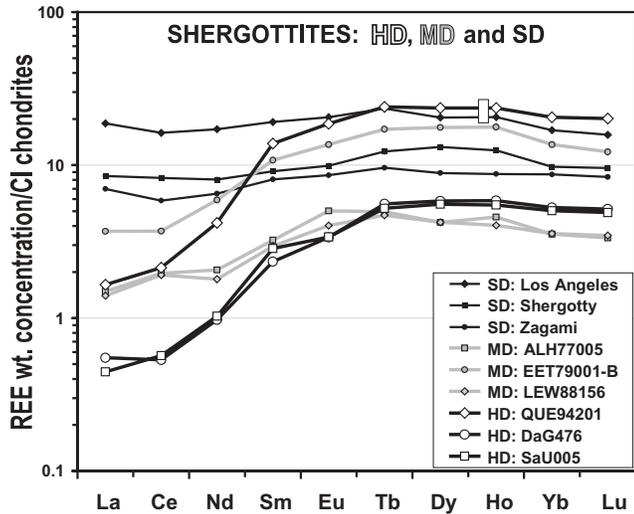
Fig. 5. CI chondrite-normalized REE patterns for basaltic shergottites. Data plotted are from the compilation of Meyer (2003) and Table 5. Patterns of the highly depleted (HD) type are extremely depleted in LREE, especially La, despite being nearly flat among the heavier REE (Tb–Lu). Patterns of the slightly depleted (SD) type are nearly flat but slightly bow-shaped, with La/Tb and Lu/Tb both c. 0.7 × CI. The moderately depleted (MD) type is intermediate.

have recognizably basaltic compositions. Mixing of 28% of the shergottite component with 54% of the *Pathfinder*, andesitic component together with lesser amounts of Mg-sulphates and ferric oxides fits the composition of martian soil analysed by the *Viking* and *Pathfinder* landers (Wänke *et al.* 2001).

Primitive and shergottite-like basalts have now also been identified at the MER 2004 landing sites (McSween & Jolliff 2004; McSween *et al.* 2004; Zipfel *et al.* 2004). 'Bounce Rock' at Meridiani Planum has 51 wt% SiO_2, 0.1 wt% K_2O and 6.5 wt% MgO (Table 4, Figs 6 and 7), and is thus similar to the basaltic shergottites. However, analyses of Gusev rocks, some of which contain large olivine crystals, have lower CaO (7.5–7.7 wt%) and higher $Na_2O + K_2O$ contents than the basaltic shergottites and a more picritic composition. Mössbauer and mini-TES spectra confirm the presence of olivine, magnetite, and probably pyroxene in the *Spirit* Gusev analyses (McSween *et al.* 2004).

The high MgO, and low CaO, TiO_2 and Al_2O_3 contents of the peridotites (Fig. 6a–c) reflect their high modal abundances of olivine grains. Similarly, the lower MgO contents of the basaltic shergottites reflect the absence of significant proportions of olivine. The olivine-phyric shergottites are intermediate in composition. The simplest explanation for the trends of negative correlation between MgO and CaO, TiO_2 and Al_2O_3 for the meteorite analyses is that the olivine-phyric shergottites are a mixture of peridotitic xenocrysts with shergottitic melt. This is the model advocated by McSween (1994) and McSween & Treiman (1998). However, as we demonstrate using La/Lu and initial [87]Sr/[86]Sr ratios of the shergottites in a later section, this is inconsistent with the geochemistry of the peridotitic shergottites (all MD) and olivine-phyric shergottites (consistently HD). Therefore even if the olivine grains within the olivine-phyric shergottites were brought in from peridotitic sources, to explain the possible mixing, they were not the same suite of peridotites as sampled within the SNC meteorites.

Goodrich (2003) proposed a more complex model than that of
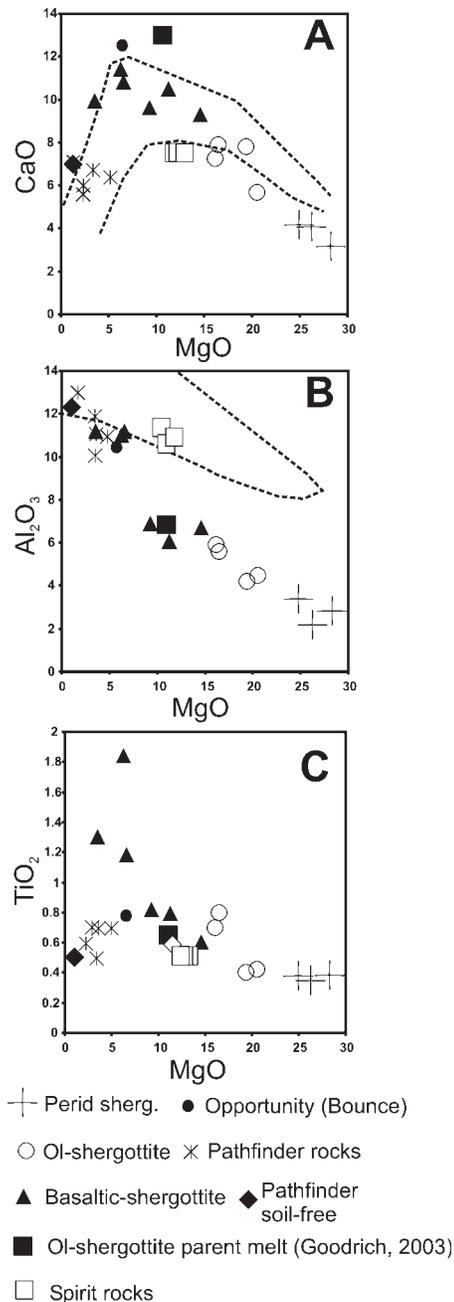
Fig. 6. Martian basalt and peridotitic shergottites compositions (wt%). (**a**) CaO v. MgO; (**b**) Al_2O_3 v. MgO; (**c**) TiO_2 v. MgO. The basaltic shergottites and *Pathfinder* analyses can be seen to have distinct compositions, *Pathfinder* analyses having lower CaO and TiO_2, and higher Al_2O_3. Also plotted are compositional fields (dashed curves) for terrestrial oceanic basalts (Basaltic Volcanism Study Project 1981). These show the generally low Al_2O_3 contents and similar CaO of most SNCs compared with terrestrial basalts. The Gusev analyses are distinct from both the basaltic and olivine shergottites, having higher MgO, and lower TiO_2 and CaO than the basaltic shergottites, but lower MgO and higher Al_2O_3 than the olivine shergottites. (See Table 4 for data sources.)

McSween & Treiman (1998). She noted that the parent magma for the large olivine grains in SaU005 (predicted from melt inclusions in chromite) was too CaO-rich to be the same as that associated with the peridotites. Therefore she proposed that in

Fig. 7. Martian basalt compositions, $Na_2O + K_2O$ v. SiO_2 (wt%). The *Pathfinder* rock and soil-free rock analyses from Wänke *et al.* (2001) and Foley *et al.* (2003) are plotted. The *Spirit* analyses (McSween *et al.* 2004) are similar to picritic basalts, whereas the *Opportunity* analysis has a higher SiO_2 content. Neither the *Spirit* nor the *Opportunity* analyses have similar compositions to the *Pathfinder* analyses. The latter have alkali-, silica-rich basaltic andesite to andesite compositions. Ol-shergottites are olivine-phyric shergottites; B. shergottites are the basaltic shergottites. Compositional fields from Cox *et al.* (1979).

addition to some material (the most Mg-rich xenocrysts or phenocrysts) that was mixed in from unidentified peridotitic sources, most of the large olivine, low-Ca pyroxene and chromite grains were derived from a separate, olivine-saturated basaltic melt. She further speculated that such a melt could have been parental to the basaltic shergottites. This idea is consistent with the work of Stolper & McSween (1979), who demonstrated with experimental phase equilibria studies of the basaltic shergottites that the primary melts from which the shergottitic melt evolved was olivine-saturated.

Figure 8 shows the phase relations of the SNCs and their associated melts in si–ol–plag space projected from wollastonite using the oxygen unit plotting parameters (equivalent to volume) of Longhi & Pan (1988) and Longhi (1991). The cumulate nakhlites, Chassigny and peridotite shergottites plot towards the olivine apex. Some of the samples (e.g. Bounce Rock and Al-rich SD shergottites) plot close to the mafic–plag cotectics, consistent with a basaltic melt rather than primarily cumulate origin. The calculated nakhlite melt of Treiman (1993) lies closest to the low-Ca px–ol cotectic, consistent with the late crystallization of plagioclase in the mesostasis of the nakhlites. The low plagioclase contents of the SNCs compared with the *Pathfinder* analyses are evident.

There is no clear link between the basaltic andesite compositions from *Pathfinder* and the basalts from shergottites and *Spirit* and *Opportunity*. However, Dann *et al.* (2001) showed that crystallization of shergottitic melts under water-saturated conditions can lead to FeO and Al_2O_3 depletion and SiO_2 enrichment to produce andesitic-like melts. In a similar set of experiments,

Minitti & Rutherford (2000) showed that 1–2 wt% H_2O in the experimental charges was necessary to produce enough melt (40 vol%) of andesitic composition to separate from the crystals.

Geochemical evidence for the importance of water in the evolution of shergottites is given by Li geochemistry. Lentz *et al.* (2001) and Beck *et al.* (2004) showed that some pyroxenes in shergottites exhibited a decrease in Li abundances from cores to rims: this was attributed to exsolution of water from the magma at depth (4–6 km). The more Li-enriched rims of some pyroxenes were attributed to their crystallization near the martian surface (<0.5 km).

The terms basaltic andesites and andesites have become widely used in the context of martian geology, and so we continue to use these terms in this paper. However, we note that for terrestrial rocks the name 'icelandite' is generally applied to those rocks of andesitic composition that formed in a nonorogenic setting. The $(NaO + K_2O)$ and SiO_2 contents of icelandites and andesites are identical (Middlemost 1985) and as no orogenic processes have ever been convincingly described on Mars the term andesite may be misleading for a martian rock (McSween *et al.* 1999).

Nakhlite and Chassigny cumulates and parental melts

The parental melt compositions of the nakhlites have been studied in a variety of ways. Treiman (1993) used electron microprobe analyses of melt inclusions and deduced that the parental melt was basaltic, rich in Fe, and poor in Al compared with terrestrial basalts (Table 4). However, Lentz *et al.* (1999) suggested that the melt had textural and compositional affinities to an Archaean ultramafic lava flow (Theo's Flow) with the exception of lower Al_2O_3 contents and Al_2O_3/CaO ratios, which reflected the Al-depleted martian mantle (e.g. Longhi 2002). Theo's Flow formed within a 120 m thick lava flow, with settling of cumulus pyroxene grains and continued growth in a growing cumulate pile, and this may be analogous to the formation conditions of the nakhlites. Melt inclusions within Chassigny olivine have also been used to calculate parental melt compositions. Like the nakhlites the calculated melt is basaltic but FeO-rich and Al_2O_3-poor with an inferred 1.5 wt% H_2O dissolved in the melt prior to kaersutite crystallization (Johnson *et al.* 1991).

In this section we show that the nakhlites formed as cumulates followed by the trapping of LREE > HREE (heavy REE) basaltic (albeit an unusually mafic and low-Al composition) melt. As shown previously, there is an almost complete overlap in augite compositions between the nakhlites ($En_{0.37-0.62}$-$Wo_{0.37-0.43}Fs_{0.24-0.41}$) but NWA817 pyroxene extends to significantly more Fe-rich compositions ($Wo_{42}En_{22-38}Fs_{20-36}$, Sautter *et al.* 2002, Fig. 4) suggesting that this nakhlite did crystallize from a more fractionated melt.

The rims (e.g. ≤20 μm in Governador Valadares, Fig. 9) are also more Fe-rich and Mg-poor than the cores. For instance, Harvey & McSween (1992) analysed a series of core–rim augite pairs in Nakhla and showed that the rims were up to $Fs_{0.6}$ in one analysis and mainly around $Fs_{0.4}$. The olivine grains within the nakhlites, apart from NWA817, are Fo_{29-38}. NWA817 olivine is Fo_{15-42} (Mikouchi *et al.* 2003) and shows zonation from core to Fe-rich rims. Thus the nakhlite olivine and the augite are not entirely in Mg–Fe equilibrium. This is shown in Figure 9a and b, X-ray maps (Fe $K\alpha$ and Mg $K\alpha$) of Governador Valadares. An explanation for this feature was provided by Harvey & McSween (1992), who suggested that olivine equilibrated more rapidly than pyroxene. However, as, for instance, Nakhla has a bulk Mg-number of 51 (Table 1, Fig. 4) the olivine has clearly not
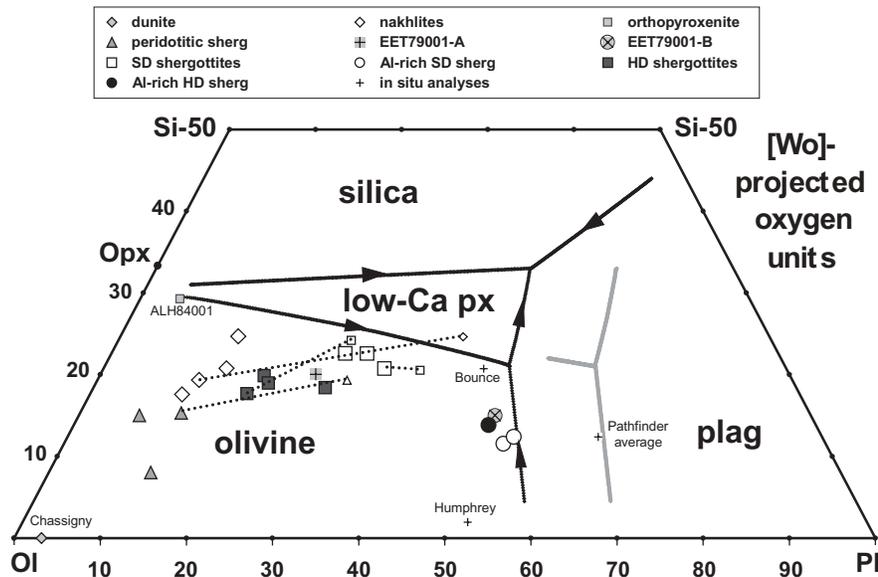
Fig. 8. Martian rock bulk compositions on the olivine–plagioclase–silica phase diagram of Longhi & Pan (1988) and Longhi (1991), based on oxygen (~ volume) units, projected from wollastonite. Conversion from molar into oxygen units is done by dividing the molar percentages by the number of oxygens in the molecular formula (four for olivine, eight for plagioclase, two for silica) and renormalizing to 100%. Boundaries shown in black are appropriate for melts with Mg-number *c.* 40–50 mol% and Na/(Na + Ca + K) *c.* 20 mol%; boundaries shown by grey lines are for higher Na/(Na + Ca + K), *c.* 40 mol% (see Longhi & Pan 1988; Longhi 1991). Meteorite compositions are based on literature data compiled by Meyer (2003), augmented by Dreibus & Jagoutz (2004) and Table 5 data for DaG476/735, SaU005, Y000593 and Y000749. In order of increasing 'Pl,' the plotted individual basaltic shergottites (blue symbols) are SaU005, DaG476, Y980459, Dhofar 019, Zagami, NWA480, Shergotty, QUE94201, Dhofar 378 and Los Angeles. Open symbols denote samples whose bulk compositions are believed to closely resemble their parent melts. Also shown (open symbols connected to meteorites by dotted lines) are modelled parent melts for Nakhla (Treiman 1993), the LEW88516 peridotitic shergottite (Harvey *et al.* 1993), SaU005 (Goodrich 2003) and Shergotty (Hale *et al.* 1999). Red crosses denote compositions obtained *in situ* by the *Pathfinder*, *Spirit* and *Opportunity* probes. The plotted *Pathfinder* compositions are the averages of five analyses (each) reported by Wänke *et al.* (2001) and Foley *et al.* (2003); as indicated in Table 2, these teams derived disparate results, particularly for SiO$_2$.

equilibrated to the bulk composition of the rock. An alternative explanation of the disequilibrium may be given by the microscopic textures. Olivine has crystallized after and around the augite cores but before their Fe-rich rims. Olivine compositions are closer to equilibrium with the final melt, rather than with the first-formed pyroxene.

The late crystallization of the olivine will also have acted to drive the composition of remaining trapped melt towards silica-oversaturated compositions. The mesostasis (which contains silica polymorphs) and the Fe-rich augite rims are the crystallized remnants of trapped melt. The proportions of trapped melt in the nakhlites are thus ≤13%, except for NWA817, which may have a higher proportion (Mikouchi *et al.* 2003). The low proportion of trapped melt is consistent with an origin for the augite grains primarily through cumulus growth, maintaining the composition of the augite, until cumulus growth ends and the trapped melt and Fe-rich rims crystallized. The mineral zonation preserved in NWA817 suggests that it underwent the least thermal equilibration of the nakhlites as a result of rapid cooling, at the top of the pile of nakhlite cumulates.

REE and fractional crystallization in the nakhlites. The petrographic model described in the previous section can be quantified through use of trace element compositions of the nakhlites. Nakhla (BM1913, 26) and Y000593 have nearly identical relative abundances of the REE (e.g. La/Lu = 3.5, 4.0; Table 6, Fig. 10). Nakhla has 4.5–1.3 × CI REE with Y000593 having slightly higher measured abundances of 6.9–1.7 × CI. The ranges of

trace element abundances of nakhlite augite and mesostasis are shown in Figure 11. The cumulus augite cores for the five nakhlites analysed have indistinguishable REE abundances with 0.5–5 × CI and La/Lu *c.* 0.75, without discernible Eu anomalies. Mesostasis analyses (containing a fine-grained mixture of glass, silica, feldspar and phosphate) reflect trapped melt compositions. They are LREE-enriched with ≤400 × CI abundances and La/Lu *c.* 14–30, generally showing smooth patterns. The lower abundances (e.g. 100 × CI La to 7 × CI Lu) for Y000593 are closest to the initial melt composition. This potential parental melt composition is similar to that calculated for Nakhla by Wadhwa & Crozaz (1995, 2003) on the basis of early-formed augite core REE abundances and a (basaltic) melt inclusion within NWA998. They suggested that the Nakhla parental melt was <60 × CI for La with La/Lu *c.* 10. The LREE > HREE smooth abundance patterns for the predicted parental melt are similar for the mesostasis with the lowest REE abundances and melt inclusion data of Wadhwa & Crozaz (2003). Here we use the Wadhwa & Crozaz data in Figure 11 to model the formation of the augite–olivine cumulates because these date have the lowest REE abundances, and so are consistent with an early, parental melt.

We use the Rayleigh fractionation equation

$$\frac{C_L}{C_o} = F^{(D-1)} \tag{1}$$

where C_L and C_o are REE concentrations within the evolving melt and original parental melt. We use a value of F (fraction of

Table 6. *Trace element abundances in the nakhlites ($\mu g\ g^{-1}$)*

	Nakhla	Y000593	Nakhla px	Nakhla px	Y000593 px	Y000593 px	Y000593 mes.	GV mes.	Calc. melt
Rb	1.29	1.77	0.51	0.13	0.00	0.00	14.2	196	
Sr	1.62	1.67	25.55	31.32	1.17	1.39	78.0	2006	
Y			3.08	4.00	0.52	0.92	16.4	56	
Zr	4.51	6.87	2.48	3.52	0.06	0.14	34.3	395	
Nb	4.58	6.70	0.13	0.18	0.09	0.08	49.1	77	
La	4.83	7.10	0.51	0.61	0.31	0.45	125.2	87	2.41
Ce	4.29	6.13	1.73	1.94	0.49	0.66	148.0	200	6.14
Pr	3.08	4.42	0.34	0.40	0.72	1.05	98.2	26	
Nd	2.50	3.56	2.00	2.31	0.83	1.32	78.7	105	3.94
Sm	2.41	3.34	0.56	0.66	0.69	1.45	45.2	18	0.82
Eu	1.92	2.67	0.19	0.19	0.72	1.00	27.6	5.9	0.21
Gd	1.86	2.56	0.74	0.77	0.62	1.09	30.3	15	0.59
Tb	1.33	1.83	0.11	0.14	0.63	1.08	22.3	1.9	
Dy	1.51	2.10	0.67	0.90	0.64	1.15	20.4	11.6	0.61
Ho	1.35	1.84	0.13	0.16	0.50	0.85	16.3	2.2	
Er	1.34	1.84	0.35	0.44	0.49	0.86	13.9	5.1	
Tm	1.28	1.74	0.05	0.07	0.45	0.86	11.5	0.6	
Yb	2.01	2.12	0.33	0.38	0.31	0.70	10.0	3.9	0.37
Lu			0.05	0.06	0.28	0.85	8.4	0.4	
Hf			0.16	0.19	0.00	0.23	29.1	10.6	

Nakhla and Y000593 are bulk analyses, others are LA-ICP-MS spot analyses on minerals; calc. melt is 10% melt added to olivine–augite cumulate (see Fig. 10 and text for details). Mes., mesostasis.

melt remaining) of 0.6 because this value is typical for ultramafic magmatic crystallization products (e.g. Snyder *et al.* 1995). The solid–melt trace element distribution coefficient D, given by

$$D = \sum w_i K_{Di} \qquad (2)$$

was calculated as the weighted mean for an unfractionated olivine (10%)–augite (90%) assemblage. This is taken to be the cumulate pile prior to final crystallization and trapping of mesostasis. Appropriate values of D for olivine and augite were taken from Papike *et al.* (1996).

The REE compositions formed from fractional crystallization of the Wadhwa & Crozaz (2003) parent melt are plotted in Figure 10. It is $100-12 \times CI$ with La/Lu *c.* 9 and a smooth abundance pattern. Addition of between 5 and 20% of this melt to the olivine–augite cumulate is consistent with the trapping of melt within the mesostasis. The profiles so formed have similar REE abundances and LREE/HREE fractionation to the nakhlite whole samples. The value of 10% is similar to the proportions of mesostasis in Nakhla and Y000593 and 20% is similar to the proportion of mesostasis in NWA817 (Mikouchi *et al.* 2003), suggesting that our model can account for the REE abundances in the nakhlites. Figure 12 (after Mikouchi *et al.* 2003) summarizes the formation of the nakhlite cumulates.

Planetary differentiation and origin of the SNC melts

The evidence for Fe-rich SNCs, the *Viking* and *Pathfinder* analyses and basalts observed on the surface with low viscosity have led to the widespread assumption (e.g. McSween 1994) that the martian mantle is Fe-rich (Table 4). The mass of the core has been estimated at 22% of the total Mars mass by Dreibus & Wänke (1985) based on SNC data. The Mars core is also assumed to be S-rich because of the depletion of chalcophile elements in SNCs (e.g. Dreibus & Wänke 1985). This small core (e.g. the Earth's is 30% by mass) is associated with a correspondingly high FeO content in the Mars mantle: 19 wt% (Mg-number *c.* 0.75) compared with 8 wt% for the Earth (Table 4). Treiman *et al.* (1987), considering the calculated abundances of side-

rophile and chalcophile elements within the mantle SNC source region, suggested that a higher range from 25 to 35% of the mass of Mars was within the core. However, the moment of inertia for Mars is now well constrained, through tracking of the *Pathfinder* lander (Folkner *et al.* 1997), at 0.3662. Bertka & Fei (1998) demonstrated that such a figure was consistent with the Fe contents suggested by Dreibus & Wänke (1985) and Lodders & Fegley (1997).

Evolution of the martian interior: late accretion and core formation

Important insight into the evolution of the martian deep interior can be obtained through highly siderophile elements (HSE), so-called because they partition strongly into metal in preference to silicate (e.g. Borisov & Palme 1995). This behaviour makes HSE sensitive recorders of core formation and of metal–silicate interactions in general. Earth's upper mantle contains moderately high levels of HSE (*c.* $0.008 \times CI$ chondrites) that are often interpreted as evidence for 'tardy' accretion of *c.* 0.5 wt% of the Earth as a chondritic 'late veneer,' subsequent to the primordial brief (or non-existent?) period of efficient core–mantle equilibration (e.g. Schmidt *et al.* 2003; Walker *et al.* 2004). The time-integrated history of accretion is one of the great unknowns of planetology, but data for lunar samples (for a recent review, see Warren 2004) and achondritic meteorites (Bogard 1995) indicate that there is a significant 'tail' effect, with a final spurt intense enough to be popularly known as a 'terminal cataclysm' at *c.* 3.85 Ga. An alternative interpretation (e.g. Righter & Drake 1997) is that during Earth's core formation extremely high pressures greatly moderated the HSE metal–silicate partition coefficients.

Of the many elements that have frequently been determined in martian meteorites, the most thoroughly siderophile are Os and Ir. In pure mafic–silicate systems, these elements show compatible behaviour, such that they tend to correlate (albeit not very tightly or linearly) with MgO (e.g. Naldrett & Barnes 1986). A plot of MgO v. Ir (Fig. 13) shows the correlation among martian meteorites (using Os in lieu of Ir would result in a nearly identical distribution). The ancient cumulate orthopyroxenite falls
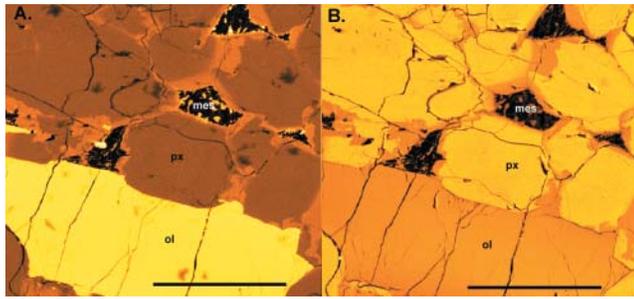
Fig. 9. X-ray maps of nakhlite (Governador Valadares) cumulate texture: (**a**) Fe Kα; (**b**) Mg Kα. The early-formed augite cores, with homogeneous compositions, are seen together with their Fe-rich and Mg-poor rims. The large olivine grain at the bottom of the figure has crystallized after the augite cores but before their Fe-rich rims. Scale bars represent 200 μm.
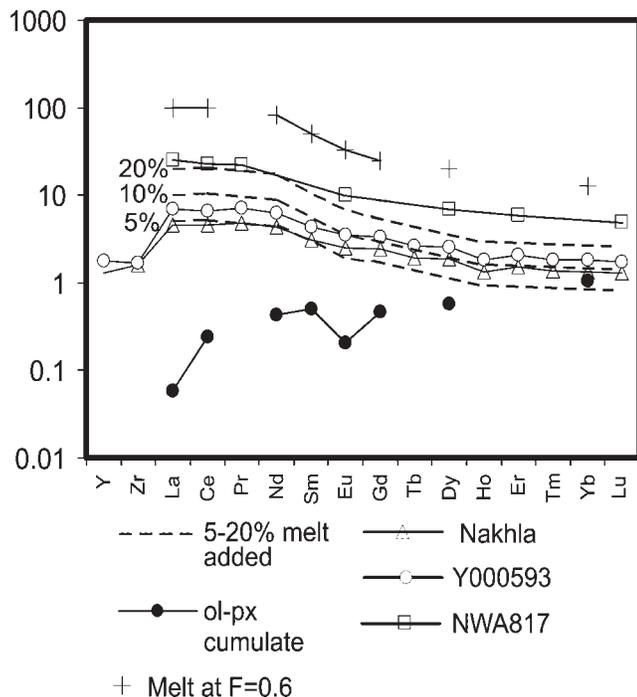

Fig. 11. Trace element abundances of nakhlite: Nakhla, Lafayette, Governador Valadares, Y000593, NWA998 minerals. Open symbols are cumulus augite, corresponding closed symbols are mesostasis (formed from trapped melt). The augite trace element abundances within the five nakhlites are indistinguishable. (See Table 6 for representative data.) Dashed line is Nakhla parent melt of Wadhwa & Crozaz (1995). Normalized to CI chondrites.

Fig. 10. REE abundances of whole Nakhla and Y000593 (Table 6) and NWA817 (Sautter *et al*. 2002) samples together with fractional crystallization model. In this model primitive olivine–augite cumulates are formed from a fractionated basaltic melt. The degree of fractional crystallization of this melt, F (i.e. fraction of melt remaining), is 0.6. The REE abundances of this melt and that of the cumulates are shown. Addition of 5–20% of this melt to the cumulate, corresponding to trapping of interstitial melt in the nakhlite mesostases, produces calculated REE abundance similar to those of the Nakhla, Y000593 and NWA817 whole samples. (See text for details of the model.) REE are normalized to CI abundances.

Fig. 12. Schematic diagram of nakhlite cumulate pile. The overall thickness, for example, in a large lava flow, is *c*. 100–200 m. NWA817 has the highest proportion of trapped, interstitial melt (light blue). This is reflected in its higher REE abundances (Fig. 9). Lafayette may have crystallized in the lowest part of the cumulate pile, as reflected by its equilibrated mineral compositions and lack of mineral zonation. Some of the augite grains show twinning on (100). NWA817 and MIL03346 have the least equilibrated olivine and pyroxene compositions. Diagram after Mikouchi *et al*. (2003).

well away from the general trend but the remaining samples show a distribution remarkably similar to that of mafic-igneous rocks from Earth. Both the Mars and Earth trends are greatly Ir enriched in comparison with the overall trend of the lunar data. In evaluating the relative positions of the trends in Figure 13, it should be recalled that Mg-number is probably roughly two times lower in the martian mantle than in the mantles of the other two

bodies; also, this Mg-number disparity is probably associated with slightly lower MgO, for an otherwise comparable martian rock, in comparison with a terrestrial or lunar counterpart. However, this is a detail, given the factor of five range in MgO among the martian meteorites. The crystalline lunar mare basalts are not obviously Ir-poor in comparison with shergottitic basalts, but the MgO-rich nonmare cumulates 67667 and 72417 indicate a major downward displacement of the lunar trend, and recent careful analyses (isotopic as well as elemental) of two types of mare-pyroclastic glass by Walker *et al.* (2004) indicate a similar, if not larger, relative depletion of HSE in the lunar mantle compared with the mantles of Mars and Earth.

These trends indicate that just like Earth, Mars retained levels of HSE in its mantle equivalent to slightly less than 1 wt% of CI-chondritic component. In contrast, the much smaller Moon managed to achieve and sustain a relatively efficient depletion of HSE from its mantle. The similarity between the HSE depletions of the martian and terrestrial mantles is a remarkable coincidence. It has occasionally been claimed (or implied) that Earth's mantle siderophile 'discrepancy' is 'unique to the Earth among all documented planetary objects' (Jana & Walker 1997); and that some peculiar trait of large planets, such as extreme pressure (e.g. Righter & Drake 1997) might account for this 'unique' evolution. It now seems clear (see Warren *et al.* 1999) that HSE behaviour in the core–mantle evolution of Mars closely paralleled HSE behaviour during evolution of Earth. Yet the pressure at the mantle–core boundary is very different in Mars (*c.* 23 GPa) and Earth (*c.* 136 GPa). Rather than an effect of
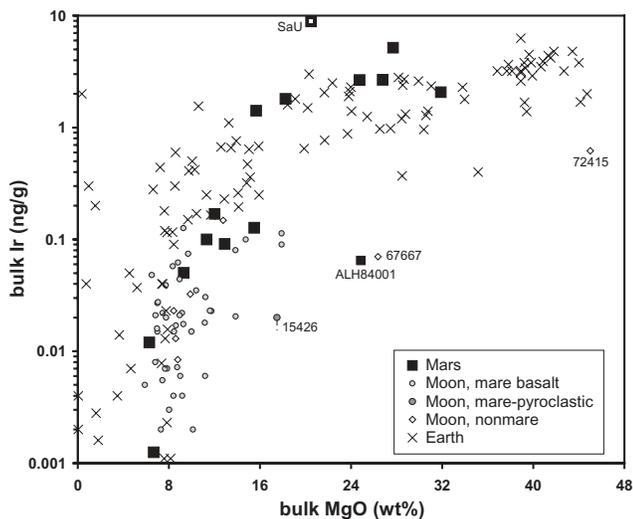

Fig. 13. Correlations between the highly siderophile element Ir and MgO for mafic igneous rocks from Mars, Earth, and the Moon. For the martian HD olivine-phyric shergottite SaU005, the plotted Ir value is the 2:1 weighted average of a direct measurement (13 ng g^{-1}: UCLA, Table 5) and an extrapolation from a vastly lower Os result (0.62 ng g^{-1}) found by Walker *et al.* (2002). The datum plotted for lunar sample 15426 (green mare-pyroclastic glass) is an upper limit (Walker *et al.* 2004). Other sources for martian data are as compiled by Meyer (2003), plusJones *et al.* (2003; excluding suspiciously high data (we suspect contamination) for ALH84001 and three shergottitic basalts) and Table 5 for the DaG735 pair of DaG476. Terrestrial and lunar background data are from sources compiled by Warren & Wasson (1979), Morgan & Wandless (1988), Ebihara *et al.* (1992) and andWarren *et al.* (1999, most notably, for the MgO-rich lunar samples 67667 and 72415).

pressure on HSE partitioning behaviour, the trends in Figure 13 might be functions of the efficiency with which late-accreted chondritic materials were stirred down into the mantle ('late' here means after the interior has cooled, from a primordial largely molten state, to the point where the mantle, being mostly solid, no longer effectively equilibrates with the core). Even after reaching a largely solid state, the Earth's mantle (as is well known) continued to convect in a style that, over time, mixes surface material with the deep interior. The post-magma-ocean Moon is and probably always has been incapable of this type of down-stirring. There are reasons to doubt that Mars ever sustained a tectonic style with Earth-like major involvement of surface plates in mantle convection (e.g. Warren 1993). But the similarity between the Mars and Earth trends in Figure 13 suggests that at least briefly in its post-core–mantle equilibration evolution, Mars sustained a style of convection or tectonism vigorous enough for it to manage (with an efficiency closer to 100% than to 0%) a sweeping of near-surface 'late' accretion matter down into its mantle.

Magma sources

The diversity of depletion characteristics among shergottites (Figs 5 and 14) shown in our geochemical classification has often been interpreted as a manifestation of varying extents of assimilative mixing between primary, HD-type basalt and a putative enriched (high La/Lu, REE-rich, Sr-rich, etc.) material (e.g. Nyquist *et al.* 2001*a*, *b*; Borg *et al.* 2002). The trace element signatures of highly diverse extents of depletion do parallel isotopic variations. For example, initial $^{87}Sr/^{86}Sr$ ratio, normalized to the typical shergottite age of 175 Ma, is consistently close to 0.701 among highly depleted shergottites, close to 0.722 among SD shergottites, and close to 0.711 among the MD shergottites (Fig. 14). A very similar pattern is manifested using ϵ_{Nd} (at 175 Ma) in lieu of initial $^{87}Sr/^{86}Sr$ (Borg *et al.* 2002).

The setting for the assimilative mixing and the detailed composition of the enriched component are speculative; the assimilated material is often referred to simply as 'crust'. Nyquist *et al.* (2001*b*) have proposed a roughly quantitative model in terms of Sr and Nd, including isotopic ratios. However, those workers did not model La/Lu (or any analogous ratio such as La/Yb). The red curve in Figure 14 shows a mixing model based on the assumptions of Nyquist *et al.* (2001*b*) for Nd, Sr and $^{87}Sr/^{86}Sr$ in the crust and HD-basalt components, augmented with an assumption that the La/Lu of the crust component was equivalent to the lunar (KREEP) crust in terms of REE pattern; that is, that it had La/Lu of 2.28 × CI chondrites (Warren 2004). This extension of the Nyquist *et al.* (2001*b*) model yields a marginally satisfactory fit to the array of shergottite compositions.

It should be noted, however, that the Nyquist *et al.* (2001*b*) model yielded (by extrapolation from all the other assumed parameters) a dubiously low Sr concentration for the HD-basalt component (specifically, 11.5–26.2 μg g^{-1}; it should be noted that only the average of 19 μg has been employed for our Fig. 14), which translates into relatively high (crust-dominated) $^{87}Sr/^{86}Sr$ at any given La/Lu position along the Figure 14 mixing curve. No known shergottite analysis has Sr <20 μg g^{-1}. The mass-weighted mean of two precise analyses for QUE94201 (Borg *et al.* 1997) is 48 μg g^{-1}, and the only other applicable result (most HD shergottites have suffered warm-desert weathering) is 20 μg g^{-1} for Y980459 (Shih *et al.* 2003). Figure 14 also includes a set of three curves based on the more realistic assumption that the average HD composition has Sr 35 μg g^{-1}.

The thick black curve is otherwise analogous to the red (19 $\mu g\,g^{-1}$) one, but the other two 35 $\mu g\,g^{-1}$ curves illustrate the sensitivity of the mixing parabolas to the assumed La/Nd and Lu/Nd (and thus La/Lu) ratios of the enriched component. In the case of the upper curve, the enriched component's REE pattern is assumed to parallel the pattern of the Earth's continental crust (Taylor 1992), with La/Lu 6.6 × CI. In the case of the lower curve, the enriched component's REE are assumed to be unfractionated ('flat') with respect to La/Lu. In all these 35 $\mu g\,g^{-1}$ models, the proportion of the enriched component that has to be added to the HD end-member to reach the SD shergottites is *c.* 17 wt%; in the 19 $\mu g\,g^{-1}$ model, it is (perhaps more realistically, from a thermophysical standpoint) *c.* 10 wt%. It should be noted that only the model with flat La/Lu comes close to matching the combination of low La/Lu and relatively high initial $^{87}Sr/^{86}Sr$ observed in the two distinct (but similar) EET79001 lithologies. An approximately flat REE pattern for an otherwise highly enriched component, although conceivable, is hardly expected as a typical outcome from planetary igneous differentiation.

Another parameter that might be at play is the enriched component's Sr level, but the 204 $\mu g\,g^{-1}$ assumed by Nyquist *et al.* agrees with an estimate of 180 $\mu g\,g^{-1}$, based on martian meteorite Sr/K systematics coupled with the *Pathfinder* soil K concentration, by Dreibus & Jagoutz (2003), albeit new data from the *Spirit* and *Opportunity* sites show only half as much soil K as was found by *Pathfinder* (Rieder *et al.* 2004). Appeal might also be made to a higher $^{87}Sr/^{86}Sr$ in the crustal component. However, Dreibus & Jagoutz (2003) argued that the $^{87}Sr/^{86}Sr$ assumed by Nyquist *et al.* (2001*b*) was already too high to represent the average crust.

Borg *et al.* (2002) extended the model of Nyquist *et al.* (2001*b*) by proposing that the crustal component was assimilated in an episode of assimilation during fractional crystallization (AFC). However, this variant of the assimilation model seems even less well-suited to account for the La/Lu constraints (Fig. 14), as the proposed fractional crystallization (including major high-Ca pyroxene) would enhance La/Lu while having no (direct) effect on the $^{87}Sr/^{86}Sr$ ratio.

In summary, it appears that a two-component mixing model (Nyquist *et al.* 2001*b*; Borg *et al.* 2002) yields a marginal fit to the MD shergottite data, but only if La/Lu in the enriched component is assumed to be KREEP-like or flatter, despite the extreme La/Lu fractionation manifested across the spectrum of SNC compositions.

Also problematic is the high proportion (probably ≫10 wt%, making realistic assumptions concerning Sr) of the enriched component that must be assimilated into the HD starting material to reach the average SD composition. Alternatively, the model may be oversimplified; MD and SD shergottites are not necessarily simple dilutions of HD matter by a single, uniform 'crust' component.

The notion of a highly depleted source region, at least for HD shergottites, and mixing with less depleted crustal matter to account for the slightly depleted (SD) shergottites such as Shergotty and Zagami, goes back at least to Nyquist *et al.* (2001*b*), and in some respects to Borg *et al.* (1997). Recent studies of shergottites (Herd *et al.* 2001, 2002; Wadhwa 2001; Goodrich *et al.* 2003; Herd 2003) have added an important new constraint by documenting a correlation between geochemical depletion or enrichment and oxygen fugacity (Fig. 15). For La/Lu, this correlation extends to the nakhlites and Chassigny. Again, despite their cumulate nature, the nakhlites and Chassigny have REE patterns (including La/Lu) lower than but roughly

parallel to the patterns of their parent melts (see above, and Wadhwa & Crozaz 1995). The quantitative fO_2 data shown for nakhlites are mainly from a recent abstract (Szymanski *et al.* 2003), but Wadhwa & Grove (2002) reported that the Gd/Eu technique yields similarly high typical fO_2 for an unspecified set of nakhlites. Chassigny's fO_2 is not yet well constrained. The fO_2 plotted in Figure 15 (QFM +0.5) is based on the spinel technique of Wood (1991; see Goodrich 2003; Herd 2003) and our own new Cr-spinel analyses; however, Chassigny's spinels may not be entirely equilibrated (Floran *et al.* 1978), so this fO_2 is only a highly approximate result, assuming a relatively high 'equilibration' *T* of 1000 °C.

It is generally assumed that the shergottites are a representative rock type in relation to the upper mantle melts (e.g. Wadhwa 2001; Herd 2003). If the relationship between depletion and fO_2 manifested among the shergottites (Fig. 15) reflects a general feature of the martian mantle–crust system, and if the spinel-derived (e.g. Herd 2003) and crystallization simulation-derived (McKay *et al.* 2002, 2004) fO_2 results are correct (Wadhwa's are systematically lower by *c.* two log units), then most of the martian upper mantle is at *c.* QFM −4 and also highly depleted.

Herd (2003) suggested that the diversity in both depletion and fO_2 among the shergottites (Figs 5 and 15) may be after-effects of a magma ocean episode. He argued that rather than reflecting mixing between primitive, reduced basaltic magmas and oxidized crust (Nyquist *et al.* 2001*b*), the depletion diversity among shergottites mainly reflects heterogeneity within the mantle, dating back to magma ocean crystallization. Herd (2003) assumed that the oxidizing component (basically Fe^{3+}) was probably closely linked with H_2O, and suggested that H_2O may have originally concentrated together with trapped melt during crystallization of the magma ocean. Herd (2003) and Treiman (2003) also noted that the H_2O-rich component in the mantle would probably become remobilized and cause complex, heterogeneous metasomatic alteration of the upper mantle. These suggestions followed a brief argument by Wadhwa & Grove (2002) that the mantle fO_2 and depletion heterogeneities formed during early differentiation because both depletion and loss of volatiles 'such as H_2O and CO_2' affected most of the mantle, but shallow regions beneath ancient cratons were exceptionally stable (against convective stirring), and these subcratonic reservoirs were subsequently 'variably metasomatized and oxidized by the melts and degassed volatiles from the deep mantle'.

The nature of the source region for the nakhlites is not certain but it is distinct from those of the shergottites. Jones (2003) suggested that the nakhlite source region represents the lower mantle; and that it stabilized below the shergottite source region because it is less depleted, and thus richer in Al_2O_3, which at mantle pressures forms dense garnet. From a physical standpoint, this seems a plausible model. Besides having more majorite, the fertile mantle would presumably be comparatively FeO-rich. Indeed, the low Mg-number of nakhlites in comparison with similarly mafic-concentrated (i.e. Al_2O_3-poor) cumulate shergottites (Fig. 16) suggests a source region considerably lower in Mg-number than the shergottite source. Density constraints reviewed by Elkins-Tanton *et al.* (2003) indicate that for a given Mg-number, majorite is *c.* 0.26 $g\,cm^{-3}$ denser than olivine (and low-Ca pyroxene; however, majorite is *c.* 0.08 $g\,cm^{-3}$ less dense than γ-olivine, the stable olivine in the *c.* 18 vol% of the martian mantle that is below *c.* 1300 km). A diminution in Mg-number of 10 mol% (as an example) translates into higher density by *c.* 0.12 $g\,cm^{-3}$, so the Mg-number effect might be even more important than a moderately higher majorite proportion in imparting negative buoyancy to a nakhlite source. An advantage

of this model is that the source is implied to be garnet-rich, and retention of even minor garnet in a restite should impart a high La/Lu to the escaping melt; yet nakhlites (and their parent melts) have La/Lu much greater than chondritic (Fig. 9).

Magma ocean and spectroscopic signatures of large-scale crustal differentiation

If a martian magma ocean (Borg & Draper 2003; Elkins-Tanton *et al*. 2003; Herd 2003; Jones 2003) existed, its end-product crust might be expected to bear some resemblance to the highly anorthositic (Al_2O_3-rich) crust that is often assumed to have formed by magma ocean plagioclase flotation on the Earth's Moon. Over most of the Moon's surface, soils have *c*. 25–28 wt% Al_2O_3 (Warren 2004), a proportion far higher than what could plausibly form by alternative models (i.e. 'serial magmatic' piecemeal emplacement of mantle-derived partial melts). However, soils at four widely separated martian sites have only about 10 wt% Al_2O_3 (Foley *et al*. 2003; Rieder *et al*. 2004). Data from orbital TES (Mars Global Surveyor: Bandfield *et al*. 2000) have been interpreted as two major compositional terranes: Type 1, basaltic (generally in the southern, older highlands) and Type 2, andesitic (generally in the northern, relatively young, low-lying plains). However, in an alternative interpretation of TES data, Wyatt *et al*. (2004) noted that there was a correlation between the Type 2 terranes and near-surface ice at middle to high latitudes. They suggested that basalt, weathered by limited inter-action with H_2O over short periods of time, could equally provide the fit rather than andesite for TES Type 2 surfaces. The geochemical evidence for basaltic andesites has been discussed previously; the modelled mineral abundances within the basaltic and andesitic spectroscopic signatures are discussed in a later section.

Orbital γ-ray spectrometry, a technique that 'sees' beneath the surface soil layer (by roughly 1 m), shows higher FeO (14–19%) in the northern lowlands than in the highlands (10–14%) (Boynton *et al*. 2004). Thus, the γ-ray data do not support the interpretation (Bandfield *et al*. 2000) that the northern crust is generally andesitic (andesites on the less FeO-rich Earth average about 7 wt% Fe: Chayes 1969). However, other aspects of the γ-ray spectrometry data (K abundances) do support the idea of andesitic material in the northern lowlands. Summing up, the spectroscopic (γ-ray and TES) evidence bearing on andesites or basaltic andesites on Mars is inconclusive. Neither the spectro-scopic data nor *in situ* soil analyses provide evidence for the preservation of early anorthositic crust.

The recent literature contains many suggestions of an early martian magma ocean (e.g. Borg & Draper 2003; Elkins-Tanton *et al*. 2003; Herd 2003), but these models seldom mention the obvious possibility that a magma ocean would have engendered an anorthositic flotation crust, as apparently happened on the Moon. Any early crust might conceivably have been recycled into the mantle, but flotation anorthosite is especially buoyant, and major involvement of surface plates in mantle convection is an unlikely scenario for Mars (e.g. Warren 1993). Borg & Draper (2003) have proposed models of martian magma ocean crystal-lization in which plagioclase flotation is a non-issue, because no plagioclase ever forms. Borg & Draper (2003) assumed that crystallization of pressure-stabilized majorite (garnet) and clin-opyroxene so depleted the melt's Al_2O_3 that it never reached saturation with plagioclase. However, based on a wealth of experimental constraints (e.g. Herzberg & Zhang 1996; Bertka & Fei 1998), igneous majorite crystallization at pressure less than (conservatively) 1 GPa is impossible. Realistically, even assum-

ing closed-system fractional crystallization at the high pressures associated with the base of the magma ocean, enough Al_2O_3 remains in the melt to eventually form many tens of kilometres (equivalent thickness) of plagioclase (Warren 1989). Further-more, the late-stage magma ocean (1) is prone to crystallize at its top as well as along its base (e.g. Morse 1982), and (2) is more realistically only the upper, fully molten subvolume of a magmasphere; that is, the melt zone is probably an open system that is replenished with fresh (and compositionally primitive) melt ascending out of the deeper interior, even during what is mainly a process of crystallization (e.g. Warren 1989).

A key parameter during crustal genesis by magma ocean plagioclase flotation is the density of the underlying melt. The melt will be saturated in pyroxene (and probably also olivine) as well as plagioclase, and the nascent crust will tend to entrain a proportion of these mafic minerals (or melt that promptly crystal-lizes mafic minerals) sufficient to impart an approximately neutral density. Warren (1990), considering a lunar magma ocean, showed that the relevant density-balance equation is

$$v_{plag} = (\rho_{maf} - \rho_{melt})/(\rho_{maf} - \rho_{plag}) \tag{3}$$

where v_{plag} is the volume fraction of plagioclase in the nascent crust, ρ_{maf} is the average density of the mafic component of the nascent crust, ρ_{melt} is the density of the melt, and ρ_{plag} is the density of the nascent plagioclase. The relevant temperature here is roughly 1200 °C, and the relevant pressure is low (even at the base of the final lunar or martian crust, only about 0.3–0.6 GPa). The low-pressure density of a silicate melt can be calculated to good precision based on its composition and the partial molar volumes of its constituent oxides (Lange & Carmichael 1990). The quantity ρ_{plag} is nearly a constant; it is slightly (0.03 g cm^{-3}) lower for a martian composition as opposed to a Na-poor lunar one. By far the most important determinant of ρ_{melt}, for the range of conceivable melt compositions, is FeO. The value of ρ_{maf} (assuming analogous varieties of mafic silicate) is also basically determined by FeO, and so is almost directly propor-tional to ρ_{melt}. Thus, to a first approximation, the volume fraction of plagioclase in the nascent crust v_{plag} is determined by one major variable, ρ_{melt}, which is in turn very largely a function of the melt FeO concentration.

The martian primitive mantle composition (constrained by geophysics as well as petrology) is fully twice as FeO-rich as the Earth's mantle (Dreibus & Wänke 1985; Bertka & Fei 1998). A disparity in Mg-number between martian rocks and analogous terrestrial mafic–ultramafic igneous rocks is obvious (Fig. 16). The martian mantle is probably also ferran in comparison with the Moon, judging from the disparate trends for cumulate or phyric samples (filled symbols) in Figure 16. Lunar regolith compositions also extrapolate to a high, Earth-like Mg-number (Warren 2004). It seems likely that FeO is higher by roughly a factor of two in the Mars crust–mantle system than in the Moon.

The relationship between initial melt FeO content and melt FeO (or ρ_{melt}) near the end of a magma ocean crystallization sequence is far more complicated than a direct proportionality. However, in the case of the lunar magma ocean, the value of ρ_{melt} can be estimated based on the observed consistently low-Mg-number and high-v_{plag} nature of the distinctive 'ferroan anorthosites' that are the only plausible representatives of a plagioclase-flotation crust (e.g. Warren 2004). The implied ρ_{melt} is roughly 2.76–2.85 g cm^{-3}, depending on whether assessed mainly based upon the observed high v_{plag} (roughly 93 vol%) implied by the ferroan anorthosites, or mainly upon forward modelling of magma ocean crystallization (Warren 1990).
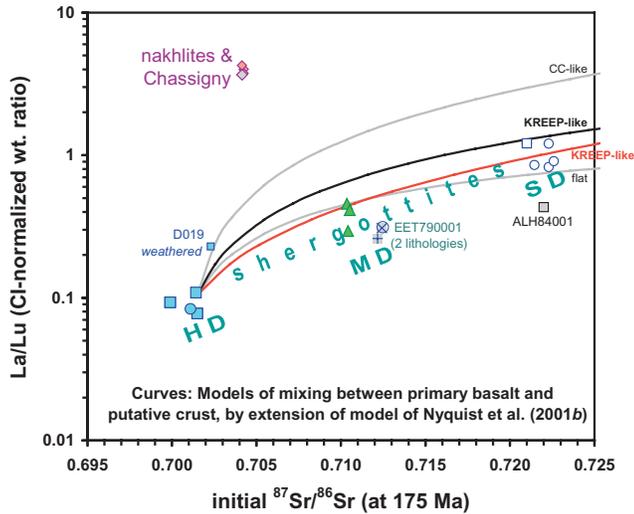
Fig. 14. Shergottites show a strong correlation, and yet a clustering into three subgroups, on a plot of La/Lu v. initial $^{87}Sr/^{86}Sr$ (normalized to a typical shergottite age of 175 Ma). Symbols are analogous to those in Figure 8. Nakhlites and Chassigny (and to a lesser extent the ancient orthopyroxenite ALH84001) plot well off the shergottite trend. Literature data used for this plot are from the same array of sources as for Figure 8. Also shown are mixing parabolas derived from four models that are discussed in the text.
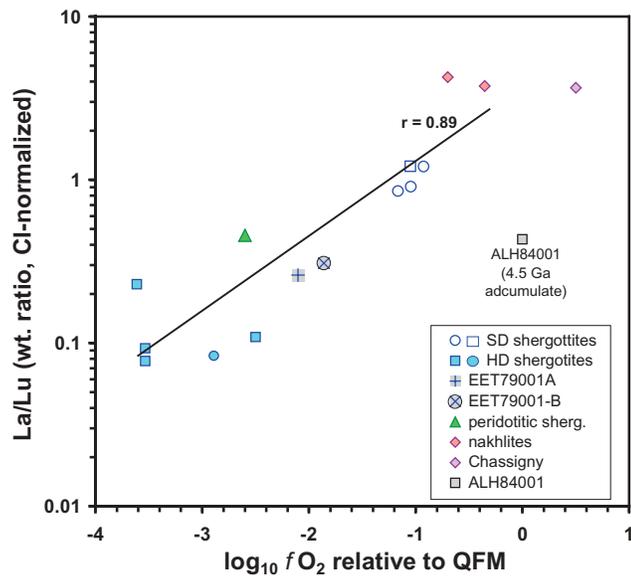
Fig. 15. Oxygen fugacity correlates with the ratio La/Lu among nearly all martian meteorites, ancient orthopyroxenite ALH84001 being a lone outlier. Symbols are analogous to those in Figure 8. Literature fO_2 data used for this plot are mainly based on opaque mineral analyses: mainly from Goodrich (2003), Herd (2003) and Szymanski et al. (2003); also Cahill et al. (2002), Warren et al. (2004), and unpublished Open University–Natural History Museum data (Table 3) for Chassigny. Caveat: fO_2 results for Chassigny and ALH84001 (Herd & Papike 1999) are only approximate. Important additional constraints on fO_2 for basaltic shergottites are available from crystallization experiments (McKay et al. 2002, 2004), and from the Gd/Eu technique of Wadhwa (2001); the Gd/Eu results tend to confirm the correlation with La/Lu, but are systematically offset from spinel-based results by about −2 log units; the technique is still undergoing calibration (McCanta et al. 2002). Data for La/Lu are from the same combination of sources as for Figure 8.
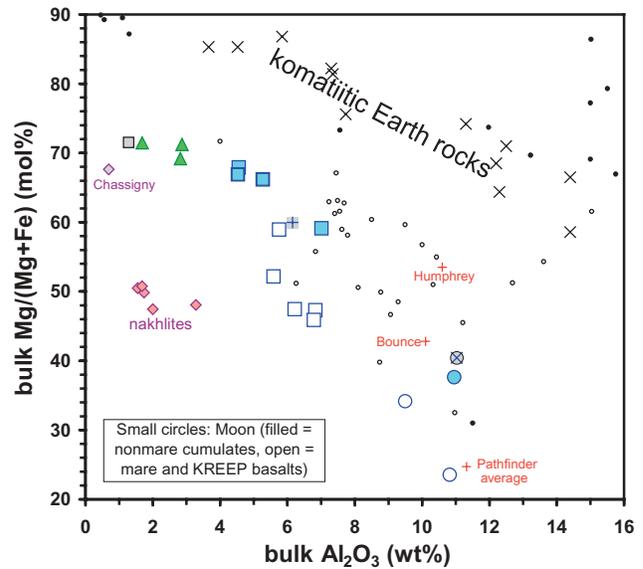

Fig. 16. Martian meteorites show systematically low Mg-number when compared with analogously mafic, Al_2O_3-poor Earth and Moon rocks. Symbols for martian samples are analogous to those in Figure 8; the single *Pathfinder* point is the average of the Wänke et al. (2001) and the Foley et al. (2003) versions of the average for five rocks. Data for martian meteorites are from the same sources as for Figure 8. Data for komatiites and komatiitic basalts are from Basaltic Volcanism Study Project (1981). Data for lunar samples are from the compilation of Warren (2004), augmented with data for lunar mare-pyroclastic glasses from Shearer & Papike (1993). The many lunar mare basalt (and pyroclastic glass) compositions shown are averages of various discrete varieties (not necessarily representing individual lavas; for example, all Apollo 12 basalts are averaged together). The two KREEP basalts shown are individual rocks (15386 and 72275; compositions from Ryder (1985) and Salpas et al. (1987)).

KREEP-basaltic melts (Ryder 1985; Salpas et al. 1987) are even less dense ($2.71–2.76 \ g \ cm^{-3}$). In the case of Mars, one approach to estimating ρ_{melt} is to assume that the late-stage magma ocean compositionally resembled the average of the four shergottites at or near plagioclase saturation (Fig. 17), which implies c. $2.81 \ g \ cm^{-3}$ (at 1200 °C, assuming $\ll 1\%$ H_2O). However, two of these shergottites are depleted (EET79001-B is MD, QUE94201 is HD), and in a very general way incompatible element depletion should correlate with FeO/MgO (i.e. melt density) depletion. Forward modelling, using assumptions analogous to those that imply c. $2.85 \ g \ cm^{-3}$ for the late lunar magma ocean, suggests a late-stage ρ_{melt} of roughly $2.85–2.94 \ g \ cm^{-3}$ (Warren 1989).

Figure 17 shows these density estimates plotted against the v_{plag} implied by equation (3), assuming a range of plausible ρ_{maf}. It would be unrealistic to expect such estimates to be accurate to much better than $0.2 \ g \ cm^{-3}$. The only reasonably confident inference is that a late-stage martian magma ocean was probably denser than its lunar counterpart, by very roughly $0.1 \ g \ cm^{-3}$. However, even this is an important inference. The implied v_{plag} is not 81–93 vol%, as in the lunar scenario, but 67–85 vol%. Even after magma ocean solidification, the same basic constraints apply: a martian crust with 76 vol% plagioclase (the nominal, mid-range result in Fig. 17) is about equally as buoyant over the dense, FeO-rich martian mantle as a lunar crust with about half as much mafic silicate (87 vol% plag) over the less dense, relatively FeO-poor lunar mantle. This moderation of the flota-
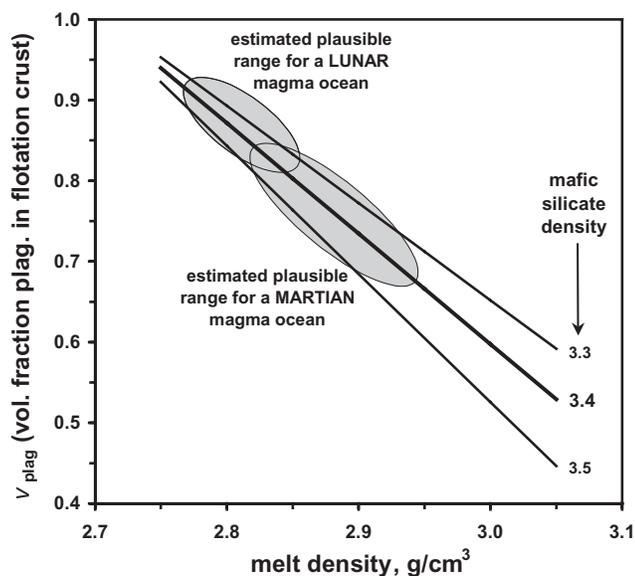
Fig. 17. Volume fraction of plagioclase v_{plag} in a magma ocean flotation crust, calculated as a function of melt density using equation (3). The high melt density expected for a late-stage martian magma ocean (see text) probably translated into a relatively moderate v_{plag}.

tion crust's composition may be part of the explanation for the lack of spectroscopic evidence for an anorthositic crustal remnant on Mars.

The existence of a magma ocean during Mars' history might account for some of the compositional features of the SNCs such as Al depletion (Al being trapped in plagioclase of the magma ocean). The fO_2 and LREE enrichments sometimes thought to be a crustal contaminant component in the shergottites might instead have resulted from magma ocean differentiation followed by a mobilization of H_2O and Fe^{3+} (Herd 2003). An alternative crustal origin for the geochemical diversity among SNCs is discussed further in relation to the source-crater locations of the SNCs.

Crystallization and ejection ages of the SNCs

The ages at which the SNC meteorites crystallized on Mars have been determined in a variety of ways including Rb–Sr, Sm–Nd and $^{39}Ar/^{40}Ar$ and these, together with Cosmic Ray Exposure (CRE) ages, have been reviewed by Nyquist *et al.* (2001a). In summary, the crystallization ages fall within five groups. ALH84001 is the oldest at 4.5 Ga, Chassigny has an age of 1.3 Ga, the nakhlites 1.3 Ga, peridotites 180 Ma and basaltic shergottites 165–475 Ma. From these ages it has been taken that ALH84001 is a fragment of Noachian crust and so probably from the southern highlands. The other 29 meteorites date from the Amazonian System, which has an age of approximately <2.9 Ga (Hartmann & Neukum 2000). These young ages of the shergottites suggest that they were derived by impacts onto the northern hemisphere and the two main likely source regions are Tharsis and Elysium–Amazonis.

The closeness of the Chassigny and nakhlite crystallization ages, which overlap within the errors, might mean that they are comagmatic, although no firmly established petrogenetic model to explain this exists. Their parental melts are both FeO-rich, Al_2O_3-poor, have LREE > HREE, and are basaltic (Johnson *et al.* 1991; Treiman 1993). Further evidence for a link between Chassigny and the nakhlites is that they both have CRE ages of

11 Ma. The CRE ages of the SNC meteorites fall within up to seven groups at 20, 15, 11, 4.5, 3, 1.3 and 0.7 Ma, leaving the possibility of seven ejection events from Mars between 20 and 0.7 Ma (Nyquist *et al.* 2001a). There is a clustering of ejection ages around 3 Ma for four of the basaltic shergottites (Los Angeles, QUE94201, Shergotty and Zagami). The peridotitic shergottites may not have been ejected in the same event; for example, LEW88516 and Y793605 were apparently ejected at 3.9 ± 0.4 Ma and 4.7 ± 0.5 Ma but the close petrographic and geochemical similarities between the peridotitic shergottites may indicate another explanation. ALH84001 has a calculated ejection age of 15 Ma.

All but one of the possible ejection events were from the northern lowlands or Tharsis. However, the ancient highlands occupy about 60% of the martian surface. Furthermore, only *c.* 12% of the martian surface is composed of lavas young enough to be associated with the shergottites (Tanaka *et al.* 1992; Keszthelyi *et al.* 2000). The reason for this over-representation of young, shergottitic material from the northern lowlands is not certain. However, it is possible that some secondary collisions in space have acted to skew the statistics and exaggerate the number of impacts on Mars that are being sampled (Nyquist *et al.* 2001a). Nyquist *et al.* and Warren & Kallemeyn (1997) also noted that uncertainty in production rates means that the distinct possibility exists, for instance, that all of the peridotitic shergottites were ejected in the same event from one crater.

Therefore the number of ejection events that have currently been sampled remains uncertain although four is a reasonable minimum estimate. Current modelling suggests that craters ⩾3 km (Head & Melosh 2000) can be associated with ejection of material from Mars at the escape velocity of 5 km s^{-1}.

Source regions and the martian surface

The young SNC ages demonstrate the existence of igneous activity on the martian surface to relatively recent times. Although, as noted previously, the high proportion of young shergottites is hard to reconcile with the martian surface there is increasing evidence, particularly from the Mars Global Surveyor camera, for young lava flows on the surface of Mars. Hartmann & Neukum (2001) conducted impact crater counts on some flows within Elysium Planitia and suggested ages of 10 Ma or less. Young lava flows (<500 Ma) cover *c.* 12% of the volcanic surface area of Mars (Keszthelyi *et al.* 2000). The potential SNC source areas in Tharsis and Elysium–Amazonis Planitia both contain lava flows thought to be <100 Ma (Hartmann & Neukum 2001). Some of the basaltic flows on Mars may be up to 1–2 km thick and extend over hundreds of square kilometres, consistent with an Fe-rich, low-viscosity nature.

Mouginis-Mark & Yoshioka (1998) studied the distribution and morphology of 59 lava flows in Elysium Planitia. They measured average widths from 3 to 16 km, with many of the flows exceeding 100 km in length. Photoclinometry was used to derive an average thickness of 40–60 m for these flows, indicating that individual flow volumes range from 18 to 70 km^3. Thus formation of nakhlites–Chassigny and perhaps the final crystallization of basaltic shergottites can potentially be accommodated within such lava flows. Peridotitic shergottites may have crystallized *in situ* as plutonic or intrusive material at deeper crustal levels.

Hamilton *et al.* (2003) reported the results of a search using TES data for spectral signatures close to those of the SNC types. Although some olivine- and orthopyroxene-rich areas were identified, no fits to the laboratory SNC spectra were found.

However, nakhlite-like materials were tentatively identified at near detection limits in the Valles Marineris area.

Bandfield *et al*. (2000) highlighted areas (e.g. Chryse and Acidalia Planitia) where what they suggested was an andesitic component (Type 2 surface) was seen. The Elysium–Amazonis and Tharsis regions do not have high detected proportions of the Type 1 or 2 end-member TES spectral signatures because the presence of surface dust precludes any useful spectra. The ancient highlands are interpreted to have a mainly basaltic signature although some areas within them (including possible source regions in Valles Marineris for the rocks on the Chryse flood plain surface) also have andesitic signatures. The spectra for the 'basaltic' signature was plagioclase 50%, augite 5%, sheet silicate 15%; for the 'andesitic' component the fit was plagioclase 35%, augite 10%, sheet silicate 15%, K-rich glass 25%. The basaltic and andesitic-like signatures dominate the surface of Mars with only relatively minor olivine-rich or haematite-rich areas. However, Hamilton *et al*. (2000, 2003) and Bibring & Erard (2001) noted that the basaltic TES spectra do not closely match those of the shergottites. Furthermore, Wyatt & McSween (2002) and Wyatt *et al*. (2004) modified the deconvolution mineralogy, significantly decreasing the estimated feldspar in both terrane types.

The calculated water contents of melt inclusions within shergottites suggest that substantial volumes of water were brought to the martian surface during the ascent and eruption of basaltic magmas. For instance, taking 1.8 wt% for the water content of an erupting basalt, then for a lava flow of 70 km^3, and a magma density of 2.85 g cm^{-3}, 3.6×10^6 m^3 of water would be released. Scott *et al*. (1998) calculated the volume of individual Tharsis shield volcanoes, including their roots, as 1.6×10^{16} m^3. This could have produced 8.2×10^{10} m^3 of water, which is *c*. 7% of the volume of the maximum north polar cap (Zuber *et al*. 1998).

We have demonstrated that conditions may have been right for the existence of a magma ocean during Mars' history. Some researchers have suggested that this magma ocean caused the geochemical heterogeneities present in the SNCs, in particular the link between LREE contents and $f O_2$ (Herd 2003). As described above, we suggest that alternative models (e.g. Nyquist *et al*. 2001*b*) based on crustal contamination do not fully account for the range of isotopic and chemical abundances present in the SNCs.

Synthesis and conclusions

The most abundant group of SNC meteorites are called the basaltic shergottites. Their composition is similar to that of rocks analysed at the *Opportunity* landing site and the basaltic component that forms much of the martian surface regolith and underlying geology in terms of Fe enrichment. However, the *Spirit* rocks are picritic and also more alkali-rich than the basaltic shergottites. Olivine-phyric shergottites form another recognizable group of the shergottites, which accumulated phenocryst or xenocryst olivine grains from a separate olivine-saturated basaltic melt. These large olivine grains were not derived by disruption of peridotite shergottite sources because the olivine-phyric shergottites generally have a more highly depleted geochemistry than the peridotitic shergottites. The six peridotite shergottites have the clearest cumulate textures of the SNCs and differ from the other shergottites in their low proportion of feldspathic material and high proportions of olivine. The cores of pyroxene in basaltic shergottites crystallized slowly at depth from melts that at least in some cases were H_2O-bearing (e.g. 4–6 km,

$\leq$1.8 wt% H_2O) followed by more rapid crystallization of the Fe-rich rims in a near-surface intrusive or extrusive setting.

The seven pyroxenite nakhlites formed as cumulates in a thick (e.g. *c*. 100 m) lava flow from the accumulation of augite followed by olivine. Trapping of varying amounts (5–20%) of basaltic, interstitial melt (the nakhlites in the upper parts of the parental lava flow having the higher proportions of trapped melt) has given the nakhlites their LREE-enriched geochemical signature. The dunite Chassigny, which has near-identical ejection and crystallization ages to the nakhlites, may also be associated with them.

The martian mantle source region has over twice the FeO contents of the terrestrial mantle and the SNC compositions reflect this in their Fe enrichment compared with analogous terrestrial and lunar rocks. Another compositional feature of the SNCs is their low Al contents, which reflect depletion of source regions, perhaps as a result of the formation of a magma ocean. However, discordance between Mg-number and Al_2O_3 contents of the nakhlite and other SNC groups shows that the SNC melts were derived from mantle source regions with differing depletion histories. The modelled martian magma ocean would have a lower proportion of plagioclase and lower density than the lunar one. Inferred noble metal contents in the martian mantle calculated from the SNCs suggest that, like the Earth, Mars underwent a later accretion of chondritic material.

In addition to petrographic classification, we suggest that the basaltic, olivine-phyric and peridotitic shergottites can also be subclassified geochemically on the basis of their LREE depletion into HD (highly depleted), MD (moderately depleted) and SD (slightly depleted). The SD shergottites mainly correspond to the basaltic shergottites, the MD to peridotitic shergottites and the HD correspond to olivine-phyric shergottites. However, LD, MD and SD all have some members from other petrological groups. This is an important classification because the La/Lu ratios (i.e. depletion) of the shergottites correlate with $\log_{10} f O_2$. The LD shergottites and also the nakhlites and Chassigny have ∆QFM of -1 to $+0.5$ and the HD shergottites have ∆QFM of -2.5 to -3.5. From these results it is inferred that the most reduced martian mantle has an oxygen fugacity of QFM -4.

The melt compositions of the SNCs, either known directly from the whole-rock composition or calculated from melt inclusions within cumulate phases, do not show any clear evidence for an andesitic component. The best data available from the *Pathfinder* rock analyses suggest that those rocks may be basaltic andesites; that is, with slightly higher SiO_2 and $Na_2O + K_2O$ than the basaltic shergottites (although it is possible that this chemistry reflects contamination of the *Pathfinder* analyses by alteration rinds). Spectroscopic data in support of the geochemical evidence for an andesitic component in the northern lowlands of Mars are not yet conclusive. However, the existence of a K- and Fe-enriched component in parts of the northern lowlands distinct from the basaltic signature in the remaining northern lowlands and southern highlands is established from TES and γ-ray spectroscopy. The formation mechanism for such large-scale magmatic heterogeneities is not clear but might involve fractionation of basaltic magmas trapped in magma ocean rocks or the fractionation of shergottitic compositions under hydrous conditions.

The absence of an andesitic-like chemical signature in the SNCs suggests that they were derived from areas in the northern lowlands where the K-rich 'andesitic' spectral signature is absent or in low abundance. Two likely regions are the Tharsis region of shield volcanoes and the Elysium–Amazonis volcanic plains. These regions also contain young volcanic rocks compatible with the relatively young ages of the SNCs. The crystallization ages fall within five groups. ALH84001 is the oldest at 4.5 Ga, the

nakhlites and Chassigny have ages of 1.3 Ga, peridotitic shergottites 180 Ma and basaltic shergottites 165–475 Ma. On the basis of these ages it is clear that only the ALH84001 orthopyroxenite is derived from the ancient highlands: this also shows the sampling bias in our current collection of 32 SNCs because *c.* 60% of the martian surface is composed of the ancient highlands. The SNCs were ejected from Mars in between four and seven impact events but uncertainties in the calculation of ejection ages means that the grouping of samples with ejection events is not always clear. However, the ejection of the nakhlites and Chassigny in one event at 11 Ma is well established.

The correlation of La/Lu with $\log_{10} f\mathrm{O}_2$ in the SNCs may be due to magma ocean-related mantle heterogeneities involved with the mobilization of H_2O and volatiles. We favour this explanation (i.e. mantle heterogeneity) over alternative explanations that the correlation is due to variable contamination with an oxidized, Sr-rich, high La/Lu hydrous fluid in crustal magma chambers. We find that mixing calculations (La/Lu v. $^{87}\mathrm{Sr}/^{86}\mathrm{Sr}$) between inferred crustal components and HD shergottite samples do not fully satisfy the range of isotopic and geochemical abundance patterns present in the SNCs.

References

Aramovich, C.J. 2002. Symplectites derived from metastable phases in martian basaltic meteorites. *American Mineralogist*, **87**, 1351–1359.

Bandfield, J., Hamilton, V. & Christensen, P. 2000. A global view of martian surface composition from MGS-TES. *Science*, **287**, 1626–1630.

Barrat, J.A., Jambon, A. & Bohn, M. et al. 2002. Petrology and chemistry of the picritic shergottite North West Africa 1068 (NWA1068). *Geochimica et Cosmochimica Acta*, **66**, 3505–3518.

Basaltic Volcanism Study Project 1981. *Basaltic Volcanism on the Terrestrial Planets*. Pergamon, New York.

Beck, P., Barrat, J.A., Chaussidon, M., Gillet, Ph. & Bohn, M. 2004. Li isotopic variations in single pyroxenes from the Northwest Africa 480 shergottite (NWA480): a record of degassing of martian magmas? *Geochimica et Cosmochimica Acta*, **68**, 2925–2933.

Berkley, J.L. & Keil, K. 1981. Olivine orientation in the ALHA77005 achondrite. *American Mineralogist*, **66**, 1233–1236.

Berkley, J.L., Keil, K. & Prinz, M. 1980. Comparative petrology of Governador Valadares and other nakhlites. *Lunar and Planetary Science Conference*, **11**, 1089–1102.

Bertka, V.M. & Fei, Y. 1998. Density profile of an SNC model Martian interior and the moment-of-inertia factor of Mars. *Earth and Planetary Science Letters*, **157**, 79–88.

Bibring, J.-P. & Erard, S. 2001. The martian surface composition. *Space Science Reviews*, **96**, 293–316.

Bogard, D.D. 1995. Impact ages of meteorites: a synthesis. *Meteoritics*, **30**, 244–268.

Bogard, D.D. & Johnson, P. 1983. Martian gases in an Antarctic meteorite? *Science*, **221**, 651–654.

Borg, L.E. & Draper, D.S. 2003. A petrogenic model for the origin and compositional variation of the martian basaltic meteorites. *Meteoritics and Planetary Science*, **38**, 1713–1731.

Borg, L.E., Nyquist, L.E., Taylor, L.A., Weismann, H. & Shih, C.-Y. 1997. Constraints on Martian differentiation processes from Rb-Sr and Sm-Nd isotopic analyses of the basaltic shergottite QUE 94201. *Geochimica et Cosmochimica Acta*, **61**, 4915–4931.

Borg, L.E., Nyquist, L.E., Wiesmann, H. & Reese, Y. 2002. Constraints on the petrogenesis of Martian meteorites from the Rb–Sr and Sm–Nd isotopic systematics of the lherzolitic shergottites ALH77005 and LEW88516. *Geochimica et Cosmochimica Acta*, **66**, 2037–2053.

Borisov, A. & Palme, H. 1995. The solubility of iridium in silicate melts: new data from experiments with Ir10Pt90 alloys. *Geochimica et Cosmochimica Acta*, **59**, 481–485.

Boynton, W., Janes, D. & Kerry, K. et al. 2004. Maps of elemental abundances on the surface of Mars (abstract). *Meteoritics and Planetary Science*, **39**, A16.

Bridges, J.C. & Grady, M.M. 2000. Evaporite mineral assemblages in the nakhlite (martian) meteorites. *Earth and Planetary Science Letters*, **155**, 183–196.

Bridges, J.C. & Grady, M.M. 2001. Chromite chemistry in SNC (martian) meteorites. *Meteoritics and Planetary Science*, **36**, A30.

Bridges, J.C., Catling, D.C., Catling, J.M., Swindle, T.D., Lyon, I.C. & Grady, M.M. 2001. Alteration assemblages in martian meteorites: implications for near-surface processes. *In:* Kallenbach, R., Geiss, J. & Hartmann, W.K. (eds) *Chronology and Evolution of Mars*. Kluwer, Dordrecht, 365–392.

Cahill, J.T., Taylor, L.A., Patchen, A., Nazorov, M.A., Stockstill, K.R. & Anand, M. 2002. Basaltic shergottite Dhofar 019: a 'normal' olivine cumulate product. *Lunar and Planetary Science Conference*, **33**, abstract 1722.

Chayes, F. 1969. The chemical composition of Cenozoic andesite. *In:* McBirney, A.R. (ed.) *Proceedings of the Andesite Conference*. Bulletin of the Oregon Department of Mineral Industries, **65**, 1–11.

Clark, B.C., Baird, A.K., Weldon, R.J., Tsusaki, D.M., Schnabel, L. & Candelaria, M.P. 1982. Chemical composition of martian fines. *Journal of Geophysical Research*, **87**, 10059–10067.

Clayton, R.N. & Mayeda, T.K. 1996. Oxygen isotope studies of achondrites. *Geochimica et Cosmochimica Acta*, **60**, 1999–2017.

Cox, K.G., Bell, J.D. & Pankhurst, R.J. 1979. *The Interpretation of Igneous Rocks*. Allen and Unwin, London.

Dann, J.C., Holzheid, A.H., Grove, T.L. & McSween, H.Y. 2001. Phase equilibria of the Shergotty meteorite: constraints on pre-eruptive water contents of martian magmas and fractional crystallization under hydrous conditions. *Meteoritics and Planetary Science*, **36**, 793–806.

Dreibus, G. & Jagoutz, E. 2003. Chemical and isotopic constraints for the martian crust. *Lunar and Planetary Science Conference*, **34**, 1350.

Dreibus, G. & Jagoutz, E. 2004. Similarities and diversities of nakhlites (abstract). *Antarctic Meteorites*, **28**, 8–9.

Dreibus, G. & Wänke, H. 1985. Mars, a volatile-rich planet. *Meteoritics*, **20**, 367–381.

Dreibus, G., Spettel, B., Haubold, R., Jochum, K.P., Palme, H., Wolf, D. & Zipfel, J. 2000. Chemistry of a new shergottite: Sayh al Uhaymir 005. *Meteoritics and Planetary Science*, **35**, A49.

Ebihara, M., Wolf, R., Warren, P.H. & Anders, E. 1992. Trace elements in 59 mostly highlands Moon rocks. *Lunar and Planetary Science Conference*, **22**, 417–426.

Elkins-Tanton, L.T., Parmentier, E.M. & Hess, P.C. 2003. Magma ocean fractional crystallization and cumulate overturn in terrestrial planets: implications for Mars. *Meteoritics and Planetary Science*, **38**, 1753–1771.

Floran, R.J., Prinz, M., Hlava, R.F., Keil, K., Nehru, C.E. & Hinthorne, J.R. 1978. The Chassigny meteorite: a cumulate dunite with hydrous amphibole-bearing melt inclusions. *Geochimica et Cosmochimica Acta*, **42**, 1213–1229.

Folco, L., Franchi, I.A., D'Orazio, M., Rocchi, S. & Schultz, L. 2000. A new Martian meteorite from the Sahara: the shergottite Dar al Gani 489. *Meteoritics and Planetary Science*, **35**, 827–839.

Foley, C.N., Economou, T. & Clayton, R.N. 2003. Final chemical results from the Mars Pathfinder alpha proton X-ray spectrometer. *Journal of Geophysical Research*, **108**, 8096.

Folkner, W.M., Yoder, C.F., Yuan, D.N., Standish, E.M. & Preston, R.A. 1997. Interior structure and seasonal mass redistribution of Mars from radio tracking of Mars Pathfinder. *Science*, **278**, 1749–1752.

Gnos, E., Hofmann, B., Franchi, I.A., Al-Kathiri, A., Hauser, M. & Moser, L. 2002. Sayh al Uhaymir 094—a new martian meteorite from the Oman desert. *Meteoritics and Planetary Science*, **37**, 835–854.

Goodrich, C.A. 2003. Petrogenesis of olivine-phyric shergottites Sayh al Uhaymir 005 and Elephant Moraine A79001 lithology A. *Geochimica et Cosmochimica Acta*, **67**, 3737–3771.

Goodrich, C.A., Herd, C.D.K. & Taylor, L.A. 2003. Spinels and oxygen fugacity in olivine-phyric and lherzolitic shergottites. *Meteoritics and Planetary Science*, **38**, 1773–1792.

Greshake, A., Fritz, J. & Stoffler, D. 2004. Petrology and shock metamorphism of the olivine-phyric shergottite Yamato 980459: evidence for a two-stage cooling and a single-stage ejection history. *Geochimica et Cosmochimica Acta*, **68**, 2359–2377.

Hale, V.P.S., McSween, H.Y. & McKay, G.A. 1999. Re-evaluation of intercumulus liquid composition and oxidation state for the Shergotty meteorite. *Geochimica et Cosmochimica Acta*, **63**, 1459–1470.

Hamilton, V., Bandfield, J. & Christensen, P. 2000. The mineralogy of martian dark regions from MGS TES data: preliminary determination of pyroxene and feldspar compositions. *Lunar and Planetary Science Conference*, **31**, abstract 1824.

HAMILTON, V.E., CHRISTENSEN, P.R., MCSWEEN, H.Y. & BANDFIELD, J.L. 2003. Searching for the source regions of martian meteorites using MGS-TES: integrating martian meteorites into the global distribution of igneous materials on Mars. *Meteoritics and Planetary Science*, **38**, 871–885.

HARTMANN, W.K. & NEUKUM, G. 2001. Cratering chronology and the evolution of Mars. *In:* KALLENBACH, R., GEISS, J. & HARTMANN, W.K. (eds) *Chronology and Evolution of Mars*. Kluwer, Dordrecht, 165–194.

HARVEY, R.P. & MCSWEEN, H.Y. 1992. Petrogenesis of the nakhlite meteorites—evidence from cumulate mineral zoning. *Geochimica et Cosmochimica Acta*, **56**, 1655–1663.

HARVEY, R.P., WADHWA, M., MCSWEEN, H.Y. JR & CROZAZ, G. 1993. Petrography, mineral chemistry and petrogenesis of Antarctic shergottite LEW88516. *Geochimica et Cosmochimica Acta*, **57**, 4769–4783.

HEAD, J.N. & MELOSH, H.J. 2000. Launch velocity distribution of the martian clan meteorites. *Lunar and Planetary Science Conference*, **31**, abstract 1937.

HERD, C.D.K. 2003. The oxygen fugacity of olivine-phyric martian basalts and the components within the mantle and crust of Mars. *Meteoritics and Planetary Science*, **38**, 1793–1805.

HERD, C.D.K. & PAPIKE, J.J. 1999. Nonstoichiometry in SNC spinels: implications for the determination of oxygen fugacity from phase equilibria. *Lunar and Planetary Science Conference*, **30**, abstract 1503.

HERD, C.D.K., PAPIKE, J.J. & BREARLEY, A.J. 2001. Oxygen fugacity of martian basalts from electron microprobe oxygen and TEM–EELS analyses of Fe–Ti oxides. *American Mineralogist*, **86**, 1015–1024.

HERD, C.D.K., BORG, L.E., JONES, J.H. & PAPIKE, J.J. 2002. Oxygen fugacity and geochemical variations in the martian basalts: implications for martian basalt petrogenesis and the oxidation state of the upper mantle of Mars. *Geochimica et Cosmochimica Acta*, **66**, 2025–2036.

HERZBERG, C. & ZHANG, J. 1996. Melting experiments on anhydrous peridotite KLB-1: compositions of magmas in the upper mantle and transition zone. *Journal of Geophysical Research*, **101**, 8271–8295.

JANA, D. & WALKER, D. 1997. The influence of silicate melt composition on distribution of siderophile elements among metal and silicate liquids. *Earth and Planetary Science Letters*, **150**, 463–472.

JOHNSON, M.C., RUTHERFORD, M.J. & HESS, P.C. 1991. Chassigny petrogenesis: melt compositions, intensive parameters and water contents of Martian(?) magmas. *Geochimica et Cosmochimica Acta*, **55**, 349–366.

JONES, J.H. 2003. Constraints on the structure of the martian interior determined from the chemical and isotopic systematics of SNC meteorites. *Meteoritics and Planet. Science*, **38**, 1807–1814.

JONES, J.H., NEAL, C.R. & ELY, J.C. 2003. Signatures of the highly siderophile elements in the SNC meteorites and Mars: a review and petrologic synthesis. *Chemical Geology*, **196**, 21–41.

KESZTHELYI, L., MCEWEN, A.S. & THORDARSON, T. 2000. Terrestrial analogs and thermal models for martian flood lavas. *Journal of Geophysical Research*, **105**, 15027–15049.

KRING, D.A., GLEASON, J.D. & SWINDLE, T.D. *ET AL.* 2003. Composition of the first bulk melt sample from a volcanic region of Mars: Queen Alexandra Range 94201. *Geochimica et Cosmochimica Acta*, **38**, 1833–1848.

LANGE, R.L. & CARMICHAEL, I.S.E. 1990. Thermodynamic properties of silicate liquids with emphasis on density, thermal expansion and compressibility. *In:* NICHOLLS, J. & RUSSELL, J.K. (eds) *Modern methods of Igneous Petrology—Understanding magmatic processes*. Mineralogical Society of America, Reviews in Mineralogy, **24**, 25–64.

LENTZ, R.C.F., TAYLOR, G.J. & TREIMAN, A.H. 1999. Formation of a martian pyroxenite: a comparative study of the nakhlite meteorites and Theo's Flow. *Meteoritics and Planetary Science*, **34**, 919–932.

LENTZ, R.F.C., MCSWEEN, H.Y., RYAN, J. & RICIPUTI, L.R. 2001. Water in martian magmas: clues from light lithophile elements in shergottite and nakhlite pyroxenes. *Geochimica et Cosmochimica Acta*, **65**, 4551–4565.

LINDSLEY, D.H., PAPIKE, J.J. & BENCE, A.E. 1972. Pyroxferroite: breakdown at low pressure and high temperature. *Lunar and Planetary Science Conference*, **3**, 483–485.

LODDERS, K. 1998. A survey of shergottite, nakhlite and chassigny meteorites whole-rock compositions. *Meteoritics and Planetary Science*, **33**, A183–A190.

LODDERS, K. & FEGLEY, B. 1997. An oxygen isotope model for the composition of Mars. *Icarus*, **126**, 1175–1182.

LONGHI, J. 1991. Complex magmatic processes on Mars—inferences from the SNC meteorites. *American Mineralogist*, **76**, 785–800.

LONGHI, J. 2002. SNC meteorites and their source compositions. *LPI Workshop on Unmixing the SNCs*. abstract 6022.

LONGHI, J. & PAN, V. 1988. A reconnaissance study of phase boundaries in low-alkali basaltic liquids. *Journal of Petrology*, **29**, 115–147.

MASON, B. 1981. ALHA77005 petrographic description. *Antarctic Meteorite Newsletter*, **4**, 12.

MCCANTA, M.C., RUTHERFORD, M.J. & JONES, J.H. 2002. An experimental study of Eu/Gd partitioning between a shergottite melt and pigeonite: implications

for the oxygen fugacity of the martian interior. *Lunar ad Planetary Science Conference*, **33**, abstract 1942.

MCCOY, T.J., TAYLOR, G.J. & KEIL, K. 1992. Zagami: product of a two-stage magmatic history. *Geochimica et Cosmochimica Acta*, **56**, 3571–3582.

MCKAY, G. & SCHWANDT, C. 2005. Mineralogy and petrology of new Antarctic nakhlite MIL03346. *Lunar ad Planetary Science Conference*, **36**, abstract 2351.

MCKAY, D.S., GIBSON, E.K. JR & THOMAS-KEPTRA, K.L. *ET AL.* 1996. Search for past life on Mars: possible biogenic activity in martian meteorite ALH84001. *Science*, **273**, 924–930.

MCKAY, G., KOIZUMI, E., MIKOUCHI, T., LE, L. & SCHWANDT, C. 2002. Crystallization of shergottite QUE 94201: an experimental study. *Lunar ad Planetary Science Conference*, **33**, abstract 2051.

MCKAY, G., LE, L., MIKOUCHI, T. & KOIZUMI, E. 2004. Redox state and petrogenesis of martian basalts: clues from experimental petrology (abstract). *Antarctic Meteorites*, **28**, 44–45.

MCSWEEN, H.Y. 1994. What we have learned about Mars from SNC meteorites. *Meteoritics*, **29**, 757–779.

MCSWEEN, H.Y. & HARVEY, R.P. 1993. Outgassed water on Mars: constraints from melt inclusions in SNC meteorites. *Science*, **259**, 1890–1892.

MCSWEEN, H.Y. & JAROSEWICH, E. 1993. Petrogenesis of the Elephant Moraine A79001 meteorite: multiple magma pulses on the shergottite parent body. *Geochimica et Cosmochimica Acta*, **47**, 1501–1513.

MCSWEEN, H.Y. & JOLLIFF, B.L. 2004. Basaltic rocks at the Meridiani and Gusev MER landing sites on Mars. *Meteoritics and Planetary Science*, **39**, A66.

MCSWEEN, H.Y. & TREIMAN, A.H. 1998. Martian meteorites. *In:* PAPIKE, J.J. (ed.) *Planetary Materials*. Mineralogical Society of America, Reviews in Mineralogy, **36**, 6-1–6-53.

MCSWEEN, H.Y., STOLPER, E.M. & TAYLOR, L.A. *ET AL.* 1979. Petrogenetic relationship between Allan Hills 77005 and other achondrites. *Earth and Planetary Science Letters*, **45**, 275–284.

MCSWEEN, H.Y., EISENHOUR, D.D., TAYLOR, L.A., WADHWA, M. & CROZAZ, G. 1996. QUE94201 shergottite: crystallization of a Martian basaltic magma. *Geochimica et Cosmochimica Acta*, **60**, 4563–4569.

MCSWEEN, H.Y., MURCHIE, S.L. & CRISP, J.A. *ET AL.* 1999. Chemical, multi-spectral, and textural constraints on the composition and origin of rocks at the Mars Pathfinder landing site. *Journal of Geophysical Research*, **104**, 8679–8715.

MCSWEEN, H.Y., ARVIDSON, R.E. & BELL, J.F. III *ET AL.* 2004. Basaltic rocks analyzed by the Spirit Rover in Gusev Crater. *Science*, **305**, 842–845.

MEYER, C. 2003. Mars meteorite compendium—2003. www-curator.jsc.nasa.gov/curator/antmet/mmc/mmc.htm.

MIDDLEMOST, E.A.K. 1985. *Magmas and Magmatic Rocks: an Introduction to Igneous Petrology.* Longman, Harlow.

MIKOUCHI, T., KOIZUMI, E., MONKAWA, A., UEDA, Y. & MIYAMOTO, M. 2003. Mineralogical comparison of Y000593 with other nakhlites: implications for relative burial depths of nakhlites. *Lunar ad Planetary Science Conference*, **34**, abstract 1883.

MIKOUCHI, T., MONKAWA, A., KOIZUMI, E., CHOKAI, J. & MIYAMOTO, M. 2005. MIL03346 nakhlite and NWA2737 ('Diderot') chassignite: two new martian cumulate rocks from hot and cold deserts. *Lunar ad Planetary Science Conference*, **36**, abstract 1944.

MINITTI, M.E. & RUTHERFORD, M.J. 2000. Genesis of the Mars Pathfinder 'sulfur-free' rock from SNC parental liquids. *Geochimica et Cosmochimica Acta*, **64**, 2535–2547.

MITTLEFEHLDT, D.W. 1994. ALH84001, a cumulate orthopyroxenite member of the martian meteorite clan. *Meteoritics*, **29**, 214–221.

MITTLEFEHLDT, D.W. 1999. An impact-melt origin for lithology A of martian meteorite Elephant Moraine A79001. *Meteoritics*, **34**, 357–367.

MORGAN, J.W. & WANDLESS, G.A. 1988. Lunar dunite 72415-72417: siderophile and volatile trace elements (abstract). *Lunar and Planetary Science Conference*, **19**, 804–805.

MORSE, S.A. 1982. Accumulus growth at the base of the lunar crust. *Lunar ad Planetary Science Conference*, **13**, A10–A18.

MOUGINIS-MARK, P. & YOSHIOKA, M.T. 1998. The long lava flows of Elysium Planitia, Mars. *Journal of Geophysical Research*, **103**, 19389–19400.

MÜLLER, W.F. 1993. Thermal and deformational history of the Shergotty meteorite deduced from clinopyroxene microstructure. *Geochimica et Cosmochimica Acta*, **57**, 4311–4322.

NALDRETT, A.J. & BARNES, S.-J. 1986. The behavior of platinum group elements during fractional crystallization and partial melting. *Fortschritte der Mineralogie*, **64**, 113–133.

NYQUIST, L.E., SHIH, C.-Y. & BOGARD, D.D. 2001a. Ages and geologic histories of martian meteorites. *In:* KALLENBACH, R., GEISS, J. & HARTMANN, W.K. (eds) *Book Title*. Kluwer, Dordrecht, 105–164.

NYQUIST, L.E., REESE, Y., WIESMANN, H. & SHIH, C.-Y. 2001b. Age of EET79001B and implications for shergottite origins. *Lunar ad Planetary Science Conference*, **32**, abstract 1407.

PAPANASTASSIOU, D.A. & WASSERBURG, G.J. 1974. Evidence for late formation and young metamorphism in the achondrite Nakhla. *Geophysical Research Letters*, **1**, 23–26.

PAPIKE, J.J., FOWLER, G.W., SHEARER, C.K. & LAYNE, G.D. 1996. Ion probe investigations of plagioclase and orthopyroxene from lunar Mg-suite norites: implications for calculating parental melt REE concentrations and for assessing postcrystallization REE redistribution. *Geochimica et Cosmochimica Acta*, **60**, 3967–3978.

PERKINS, W.T., PEARCE, N.J.G. & JEFFRIES, T.E. 1993. Laser ablation inductively coupled plasma mass-spectrometry – a new technique for the determination of trace and ultra-trace elements in silicates. *Geochimica et Cosmochimica Acta*, **57**, 475–482.

PRINZ, M., HLAVA, P.H. & KEIL, K. 1974. The Chassigny meteorite: a relatively iron-rich cumulate dunite (abstract). *Meteoritics*, **9**, 393–394.

REID, A.M. & BUNCH, T.E. 1975. The nakhlites, part II: where, when, and how. *Meteoritics*, **10**, 317–324.

RIEDER, R., GELLERT, R. & BRÜCKNER, J. ET AL. 2004. APXS on Mars: analyses of soils and rocks at Gusev Crater and Meridiani Planum. *Lunar ad Planetary Science Conference*, **35**, abstract 2172.

RIGHTER, K. & DRAKE, M.J. 1997. Metal–silicate equilibrium in a homogeneously accreting Earth: new results for Re. *Earth and Planetary Science Letters*, **146**, 541–553.

RUBIN, A.E., WARREN, P.H. & GREENWOOD, J.P. ET AL. 2000. Los Angeles: the most differentiated basaltic Martian meteorite. *Geology*, **28**, 1011–1014.

RYDER, G. 1985. *Catalog of Apollo 15 Rocks*. NASA Johnson Space Center, Houston, Curatorial Publication, **20787**.

SALPAS, P.A., TAYLOR, L.A. & LINDSTROM, M.M. 1987. Apollo 17 KREEPy basalts: evidence for the nonuniformity of KREEP. Proceedings of the 17th Lunar and Planetary Science Conference. *Journal of Geophysical Research*, **92**, E340–E348.

SAUTTER, V., BARRAT, J.A. & JAMBON, A. ET AL. 2002. A new martian meteorite from Morocco: the nakhlite North West Africa 817. *Earth and Planetary Science Letters*, **195**, 223–238.

SCHMIDT, G., WITT-EICKSCHEN, G., PALME, H., SECK, H., SPETTEL, B. & KRATZ, K.-L. 2003. Highly siderophile elements (PGE, Re and Au) in mantle xenoliths from the West Eifel volcanic field (Germany). *Chemical Geology*, **196**, 77–105.

SCOTT, E.D., WILSON, L. & HEAD, J.W. 1998. Episodicity in the evolution of the large Tharsis volcanoes. *Lunar ad Planetary Science Conference*, **29**, abstract 1353.

SHEARER, C.K. & PAPIKE, J.J. 1993. Basaltic magmatism on the Moon—a perspective from volcanic picritic glass beads. *Geochimica et Cosmochimica Acta*, **57**, 4785–4812.

SHIH, C.-Y., NYQUIST, L.E. & WIESMANN, H. 2003. Isotopic studies of Antarctic olivine-phyric shergottite Y980459 (abstract). *In: International Symposium: Evolution of Solar System Materials: a New Perspective from Antarctic Meteorites*. National Institute of Polar Research, Tokyo, 125–126.

SNYDER, G.A., NEAL, C.R. & TAYLOR, L.A. 1995. Processes involved in the formation of magnesian-suite plutonic rocks from the highlands of the Earth's Moon. *Journal of Geophysical Research*, **100**, 9365–9388.

STOLPER, E.M. 1979. Trace elements in shergottite meteorites: implications for the origins of planets. *Earth and Planetary Science Letters*, **42**, 239–242.

STOLPER, E.M. & MCSWEEN, H.Y. 1979. Petrology and origin of the shergottite meteorites. *Geochimica et Cosmochimica Acta*, **43**, 1475–1498.

SZYMANSKI, A., BRENKER, F.E., EL GORESY, A. & PAL, H. 2003. Complex thermal history of Nakhla and Y000593. *Lunar and Planetary Science Conference*, **34**, abstract 1922.

TANAKA, K.L., SCOTT, D.H. & GREELEY, R. 1992. Global stratigraphy. *In: KIEFFER, H.H. ET AL. (ed.) Mars*. University of Arizona Press, Tucson, 345–382.

TAYLOR, S.R. 1992. *Solar System Evolution a New Perspective*. Cambridge University Press, Cambridge.

TREIMAN, A.H. 1985. Amphibole and hercynite spinel in Shergotty and Zagami: magmatic water, depth of crystallization, and metasomatism. *Meteoritics*, **20**, 229–243.

TREIMAN, A.H. 1993. The parent magma of the Nakhla (SNC) Meteorite, inferred from magmatic inclusions. *Geochimica et Cosmochimica Acta*, **57**, 4753–4767.

TREIMAN, A.H. 1995. A petrographic history of martian meteorite ALH84001: two shocks and an ancient age. *Meteoritics*, **30**, 294–302.

TREIMAN, A.H. 2003. Chemical compositions of martian basalts (shergottites): some inferences on basalt formation, mantle metasomatism, and differentiation on Mars. *Meteoritics and Planetary Science*, **38**, 1849–1864.

TREIMAN, A.H., JONES, J. & DRAKE, M.J. 1987. Core formation in the shergottite parent body and comparison with Earth. *Journal of Geophysical Research*, **92**, E627–E632.

TURCOTTE, D.L. & SCHUBERT, G. 1982. *Geodynamics: Applications of Continuum Physics to Geological Problems*. Wiley, New York.

VAN NIEKERK, D., GOODRICH, C.A., TAYLOR, G.J. & KEIL, K. 2005. Characterization of the lithological contact in the Shergottite EETA79001. *Meteoritics and Planetary Science*, **39**, A108.

WADHWA, M. 2001. Redox state of Mars' upper mantle and crust from Eu anomalies in shergottite pyroxenes. *Science*, **291**, 1527–1530.

WADHWA, M. & CROZAZ, G. 1995. Trace and minor elements in minerals of nakhlites and Chassigny: clues to their petrogenesis. *Geochimica et Cosmochimica Acta*, **59**, 3629–3645.

WADHWA, M. & CROZAZ, G. 2003. Trace element geochemistry of new nakhlites from the Antarctic and the Saharan Desert: further constraints on nakhlite petrogenesis on Mars. *LPS*, **34**, abstract 2075.

WADHWA, M. & GROVE, T.L. 2002. Archean cratons on Mars? Evidence from trace elements, isotopes and oxidation states of SNC magmas. *Geochimica et Cosmochimica Acta*, **66**, A816.

WADHWA, M., MCSWEEN, H.Y. & CROZAZ, G. 1994. Petrogenesis of shergottite meteorites inferred from minor and trace element microdistributions. *Geochimica et Cosmochimica Acta*, **58**, 4213–4229.

WADHWA, M., CROZAZ, G., TAYLOR, L.A. & MCSWEEN, H.Y. 1998. Martian basalt (shergottite) QUE94201 and lunar basalt 15555: a tale of two pyroxenes. *Meteoritics and Planetary Science*, **33**, 321–328.

WALKER, R.J., BRANDON, A.D., NAZAROV, M.A., MITTLEFEHLDT, D., JAGOUTZ, E. & TAYLOR, L.A. 2002. ^{187}Re–^{187}Os isotopic studies of SNC meteorites: an update. *Lunar ad Planetary Science Conference*, **33**, abstract 1042.

WALKER, R.J., HORAN, M.F., SHEARER, C.K. & PAPIKE, J.J. 2004. Low abundances of highly siderophile elements in the lunar mantle: evidence for prolonged late accretion. *Lunar ad Planetary Science Conference*, **35**, abstract 1110.

WÄNKE, H. 1968. Radiogenic and cosmic-ray exposure ages of meteorites, their orbits and parent bodies. *In: AHRENS, L.H. (ed.) Origin and Distribution of the Elements*. Pergamon, Oxford, 411–421.

WÄNKE, H., BRÜCKNER, J., DREIBUS, G., RIEDER, R. & RYABCHIKOV, I. 2001. Chemical composition of rocks and soils at the Pathfinder site. *Space Science Reviews*, **96**, 317–330.

WARREN, P.H. 1989. Growth of the continental crust, a planetary-mantle perspective. *Tectonophysics*, **161**, 165–199.

WARREN, P.H. 1990. Lunar anorthosites and the magma-ocean plagioclase-flotation hypothesis: importance of FeO enrichment in the parent magma. *American Mineralogist*, **75**, 46–58.

WARREN, P.H. 1993. The magma ocean as an impediment to lunar plate tectonics. *Journal of Geophysical Research—Planets*, **98**, 5335–5345.

WARREN, P.H. 2004. The Moon. *In: DAVIS, A.M. (ed.) Treatise on Geochemistry, Volume 1, Meteorites, Comets, and Planets*. Elsevier–Pergamon, Oxford, 559–599.

WARREN, P.H. & KALLEMEYN, G.W. 1997. Yamato-793605, EET79001, and other presumed martian meteorites: compositional clues to their origins. *Antarctic Meteorite Research*, **10**, 61–81.

WARREN, P.H. & WASSON, J.T. 1979. The compositional–petrographic search for pristine nonmare rocks—third foray. *Proceedings of the 10th Lunar and Planetary Science Conference*, 583–610.

WARREN, P.H., KALLEMEYN, G.W. & KYTE, F.T. 1999. Origin of planetary cores: evidence from highly siderophile elements in martian meteorites. *Geochimica et Cosmochimica Acta*, **63**, 2105–2122.

WARREN, P.H., GREENWOOD, J.P. & RUBIN, A.E. 2004. Los Angeles: a tale of two stones. *Meteoritics and Planetary Science*, **39**, 137–156.

WATSON, L.L., HUTCHEON, I.D., EPSTEIN, S. & STOLPER, E.M. 1994. Water on Mars—clues from deuterium/hydrogen and water contents of hydrous phases in SNC meteorites. *Science*, **265**, 86–90.

WOOD, B.J. 1991. Oxide barometry of spinel peridotites. *In: LINDSLEY, D.H. (ed.) Oxide Minerals: Petrologic and Magnetic Significance*. Mineralogical Society of America, Reviews in Mineralogy, **25**, 417–431.

WOOD, C.A. & ASHWAL, L.D. 1981. SNC meteorites: igneous rocks from Mars? *Proceedings of Lunar and Planetary Science*, **12B**, 1359–1375.

WYATT, M.B. & MCSWEEN, H.Y. 2002. Spectral evidence for weathered basalt as an alternative to andesite in the northern lowlands of Mars. *Nature*, **417**, 263–266.

WYATT, M.B., MCSWEEN, H.Y., TANAKA, K.L. & HEAD, J.W. 2004. Global geologic context for rock types and surface alteration on Mars. *Geology*, **32**, 645–648.

ZIPFEL, J., ANDERSON, R. & BRUCKNER, J. ET AL. 2004. APXS analyses of Bounce rock—the first shergottite on Mars. *Meteoritics and Planetary Science*, **39**, 5173.

ZUBER, M.T., SMITH, D.E. & SOLOMON, S.C. ET AL. 1998. Observations of the north polar region of Mars from the Mars Orbiter Laser Altimeter. *Science*, **282**, 2053–2060.